Carbon Scrape-Off Layer Transport and Deposition in DIII-D

By
M. Groth*

S.L. Allen,* M.E. Fenstermacher,* C.J. Lasnier,* G.D. Porter,*
M.E. Rensink,* T.D. Rognlien,* J.A. Boedo,[†] D.L. Rudakov,[†]
N.H. Brooks,[‡] R.J. Groebner,[‡] A.W. Leonard,[‡] W.P. West.[‡]
J.D. Elder,[△] S. Lisgo,[△] A.G. McLean,[△] P.C. Stangeby,[△]
W.R. Wampler,[§] J.G. Watkins,[§] D.G. Whyte,[#]

*Lawrence Livermore National Laboratory, Livermore, CA
[†]University of California San Diego, La Jolla, CA
[‡]General Atomics, San Diego, CA
[△]University of Toronto (UTIAS), Toronto, Ontario, Canada
[§]Sandia National Laboratory, Albuquerque, NM, USA
[#]Massachusetts Institute of Technology, Cambridge, MA

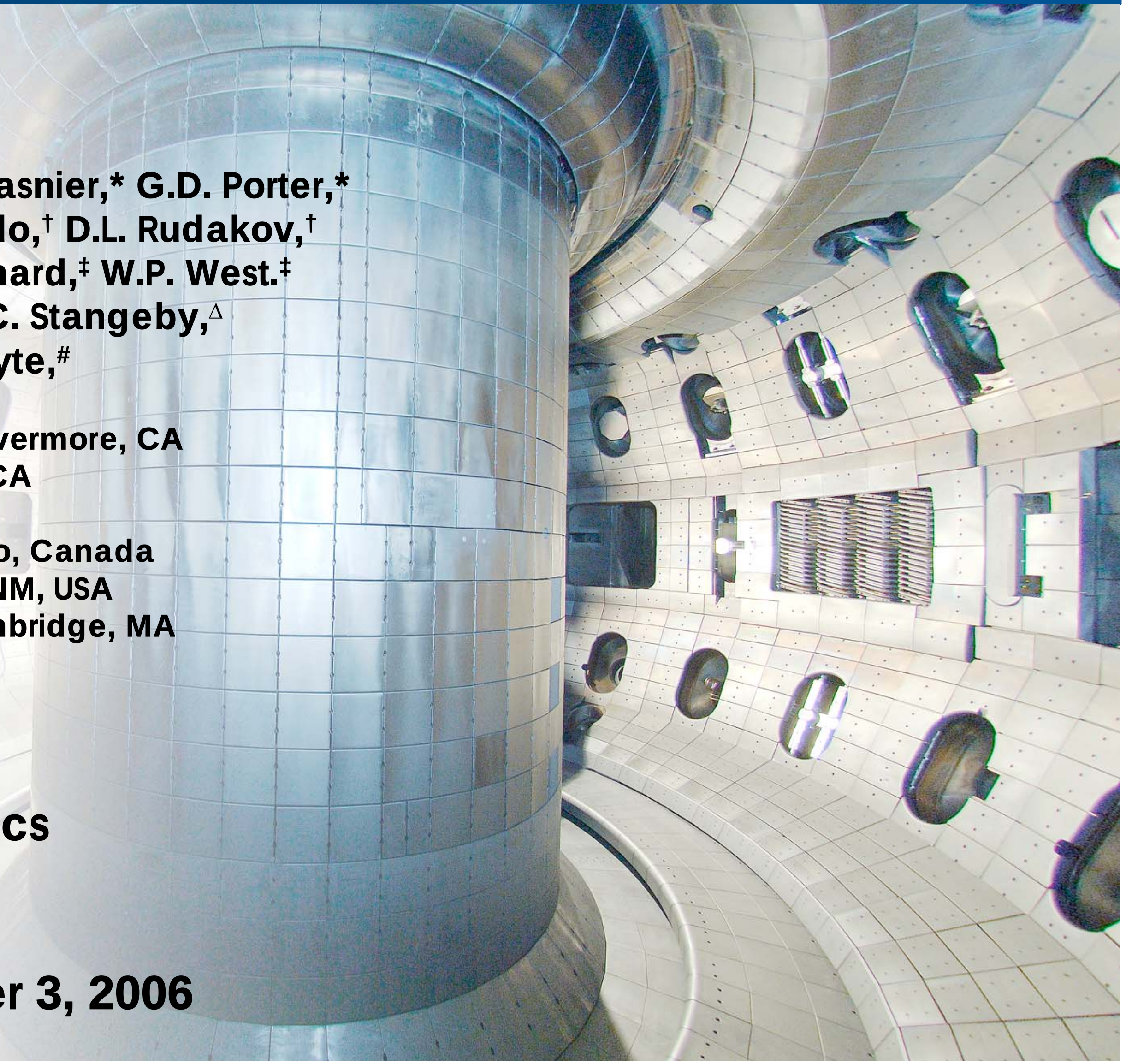

**Presented at the
48th Annual Meeting
of the Division of Plasma Physics
Philadelphia, Pennsylvania**

October 30 through November 3, 2006

Tritium Retention Due to Co-deposition With Carbon Potentially Limits Duty Cycle of Future Fusion Reactors

JET

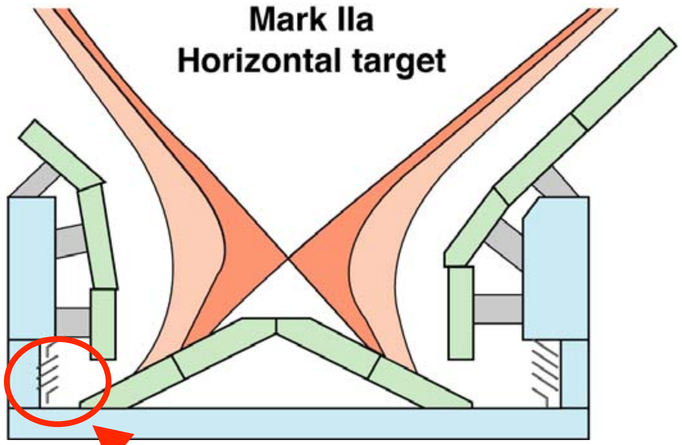

Tritium-rich carbon deposits in JET inner divertor

- **Tritium retention in fusion devices occurs via carbon co-deposition**
- **JET deuterium-tritium campaign showed strong tritium accumulation in plasma-shadowed regions**

⇒ **What is the primary source of carbon deposited at the inner divertor?**

⇒ **What are the transport mechanisms involved?**

Sources of Carbon in DIII-D Are Distributed Between the Main Chamber and the Divertor Walls

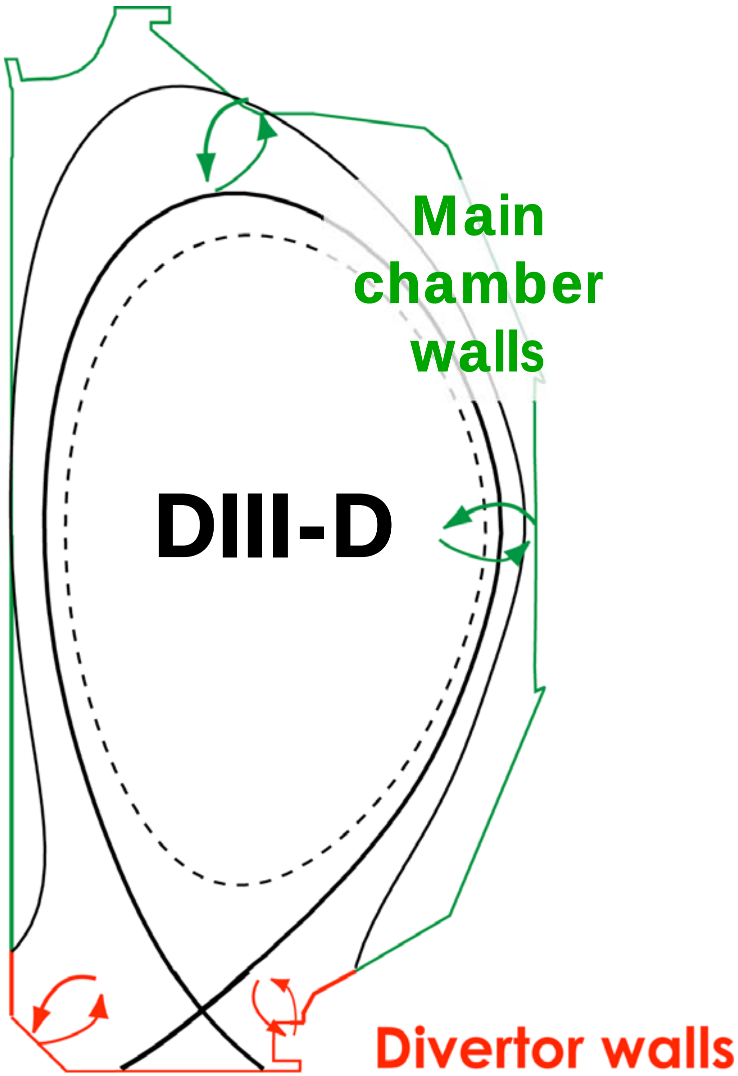

- **Relative source contribution depends on tokamak operation**
  - Heating power
  - Upstream density
  - Separation of confined plasma from main chamber walls
- **Divertor dominant source in low-to-moderate density regimes**
- **Main chamber walls are significant contributor in high-density regimes**

Carbon Deposition in the Divertor Depends on Scrape-off Layer Transport and Divertor Plasma Conditions

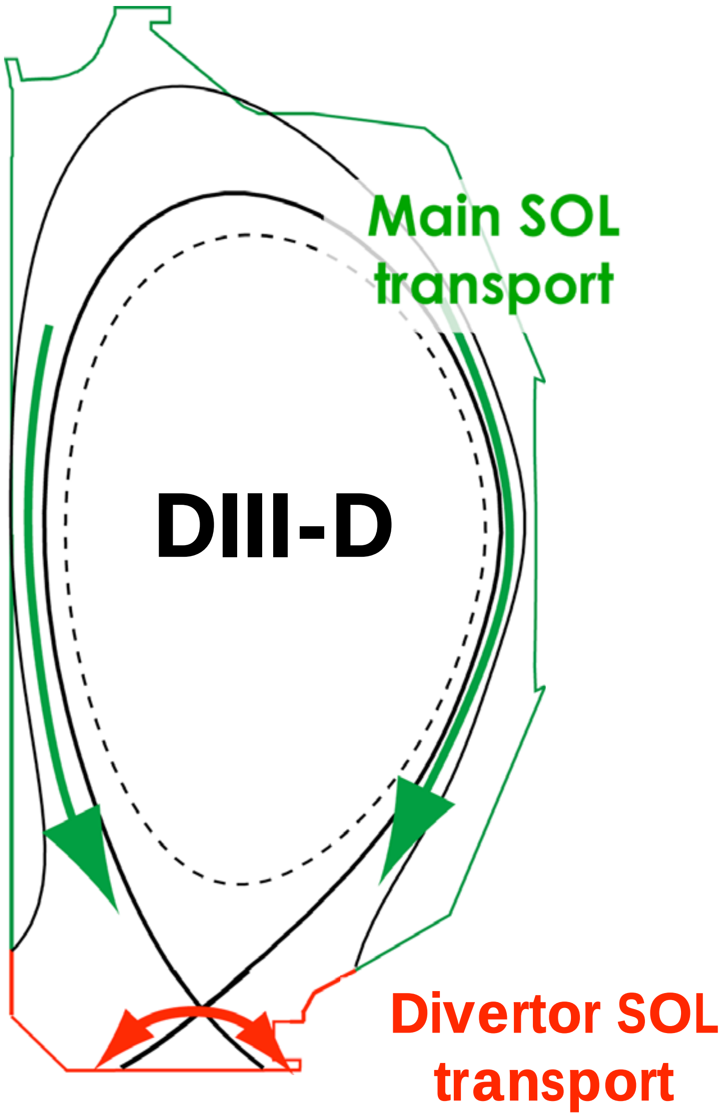

- **Carbon transport determined by coupling to hydrogen SOL flows and drifts**
- **In the divertor, carbon deposition occurs predominately along surfaces exposed to detached (T < 3 eV) plasmas**

Toroidally Localized Methane Injection From the Main Wall and Outer Divertor Produces Deposition at the Inner Divertor

- **Use isotope ^{13}C in hydrated methane as marker on ^{12}C graphite tiles for surface analysis**

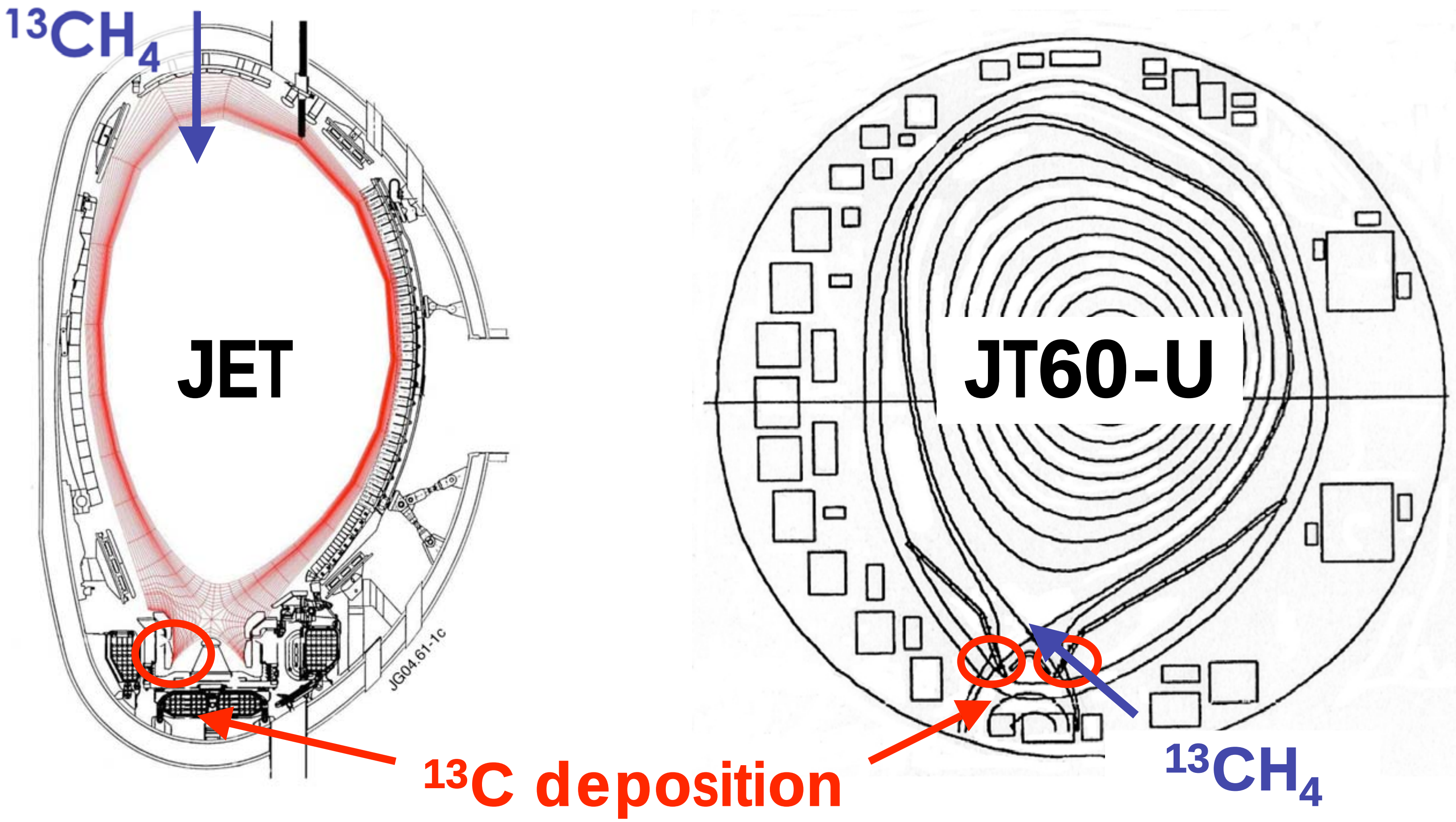

Transport and Deposition of Carbon From the Main Chamber Walls Were Investigated in DIII-D by Methane Injection

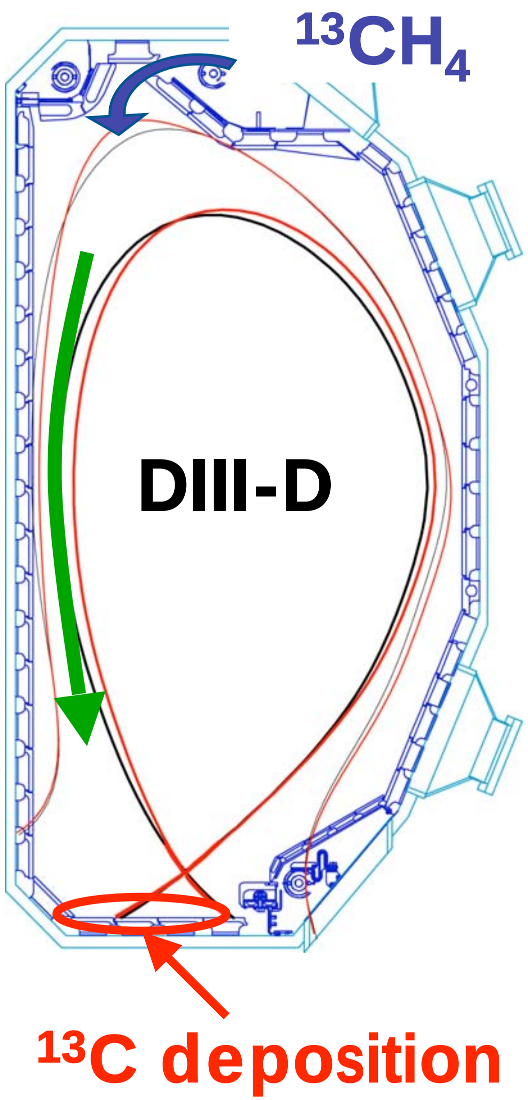

- Toroidally symmetric $^{13}CH_4$ injection into L-mode and H-mode plasmas
- ^{13}C surface analysis: highest ^{13}C concentration along surfaces exposed to cold divertor plasmas
- Carbon transport from the crown to the inner divertor via frictional coupling to deuteron flow
- Carbon transport and deposition simulations

Transport and Deposition of Carbon From the Main Chamber Walls Were Investigated in DIII-D by Methane Injection

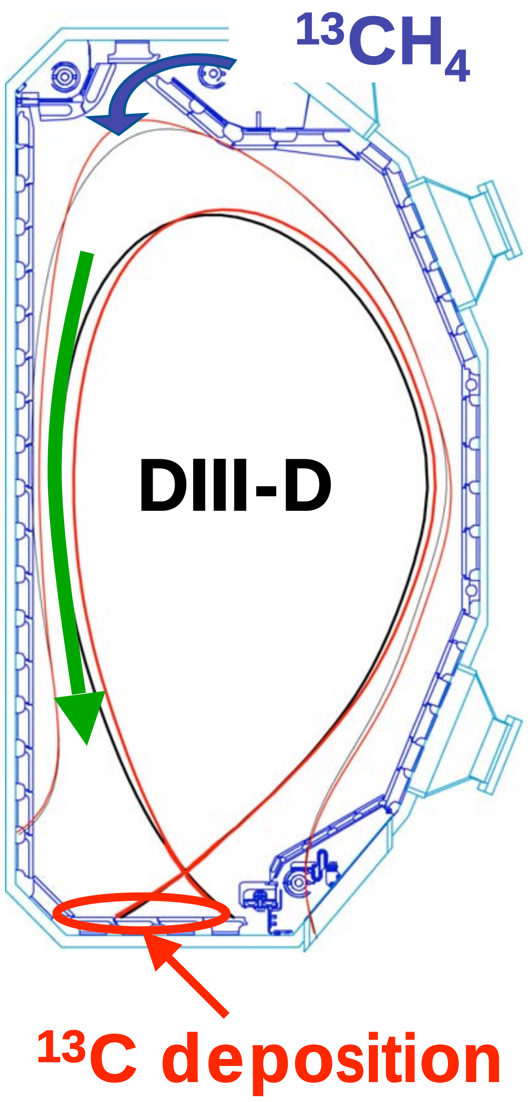

- **Toroidally symmetric $^{13}CH_4$ injection into L-mode and H-mode plasmas**
- **^{13}C surface analysis: highest ^{13}C concentration along surfaces exposed to cold divertor plasmas**
- **Carbon transport from the crown to the inner divertor via frictional coupling to deuteron flow**
- **Carbon transport and deposition simulations**

Carbon Transport Studies in DIII-D Lower Single Null Low-density L-mode and High-density H-mode Plasmas

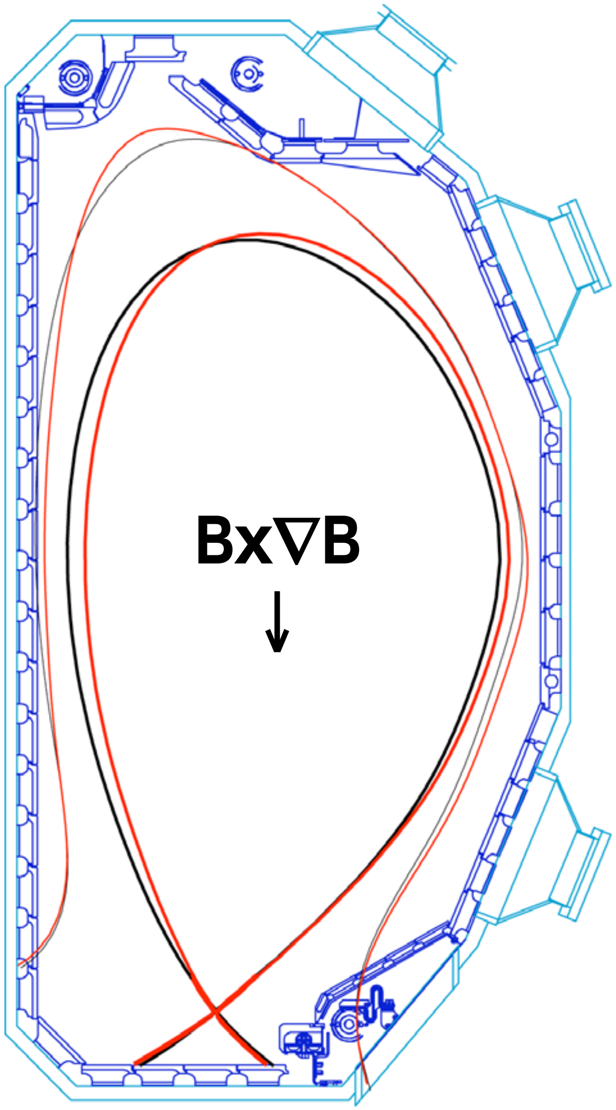

Plasma / Param.	L-mode	ELMy H-mode
Campaign	2003	2005
$\langle n_e \rangle$ [m-3]	$3\text{x}10^{19}$	$8\text{x}10^{19}$
P_{NBI} [MW]	0.2	6.6
$T_{e,ISP}$ [eV]	< 2 cold	< 2 detached
$T_{e,OSP}$ [eV]	25 attached	< 2 detached
		ELMing @ 200 Hz

Inner and Outer Divertor Plasmas Were Attached in L-mode

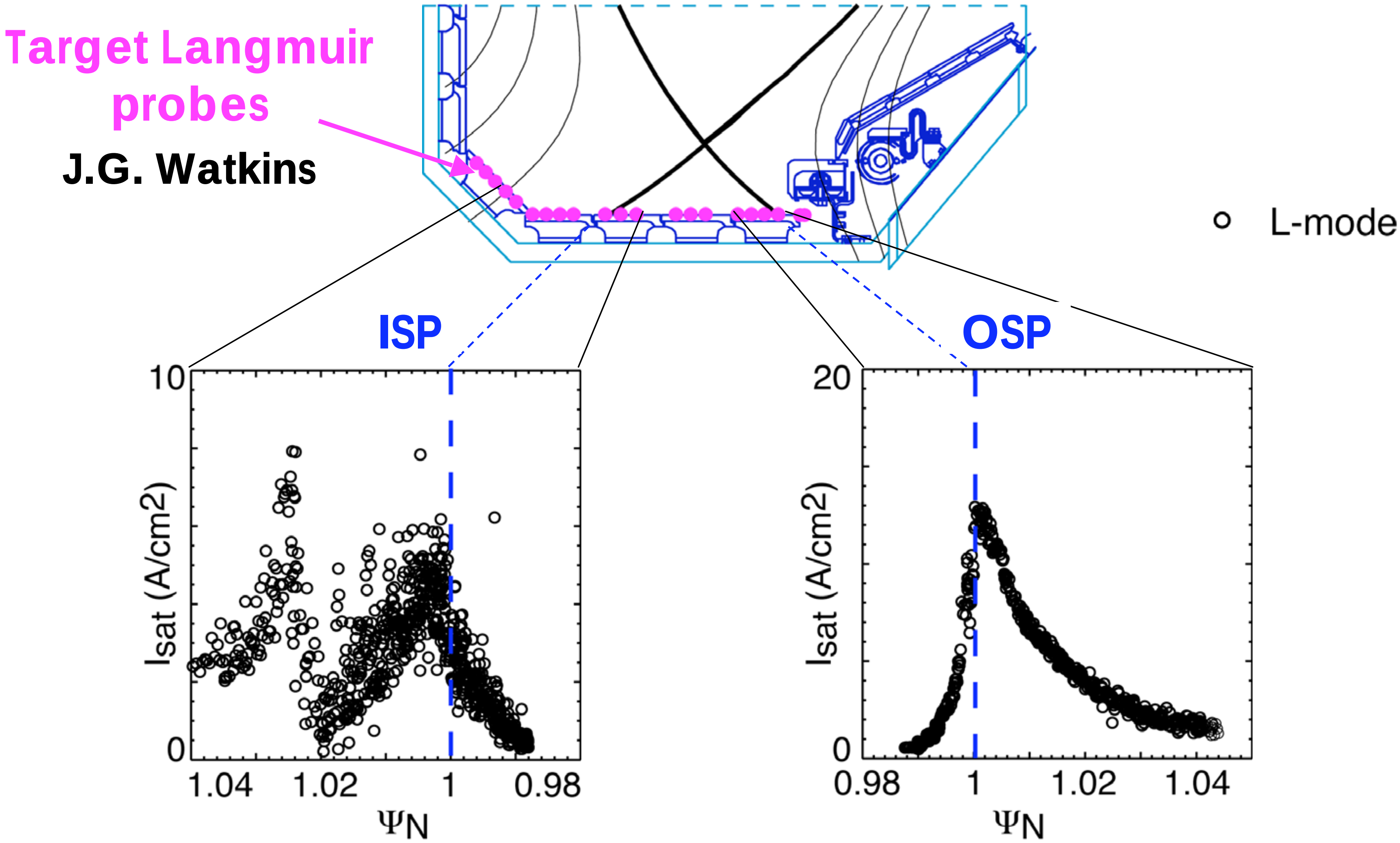

Inner and Outer Divertor Plasmas Were Attached in L-mode, but Detached in H-mode Between Elms

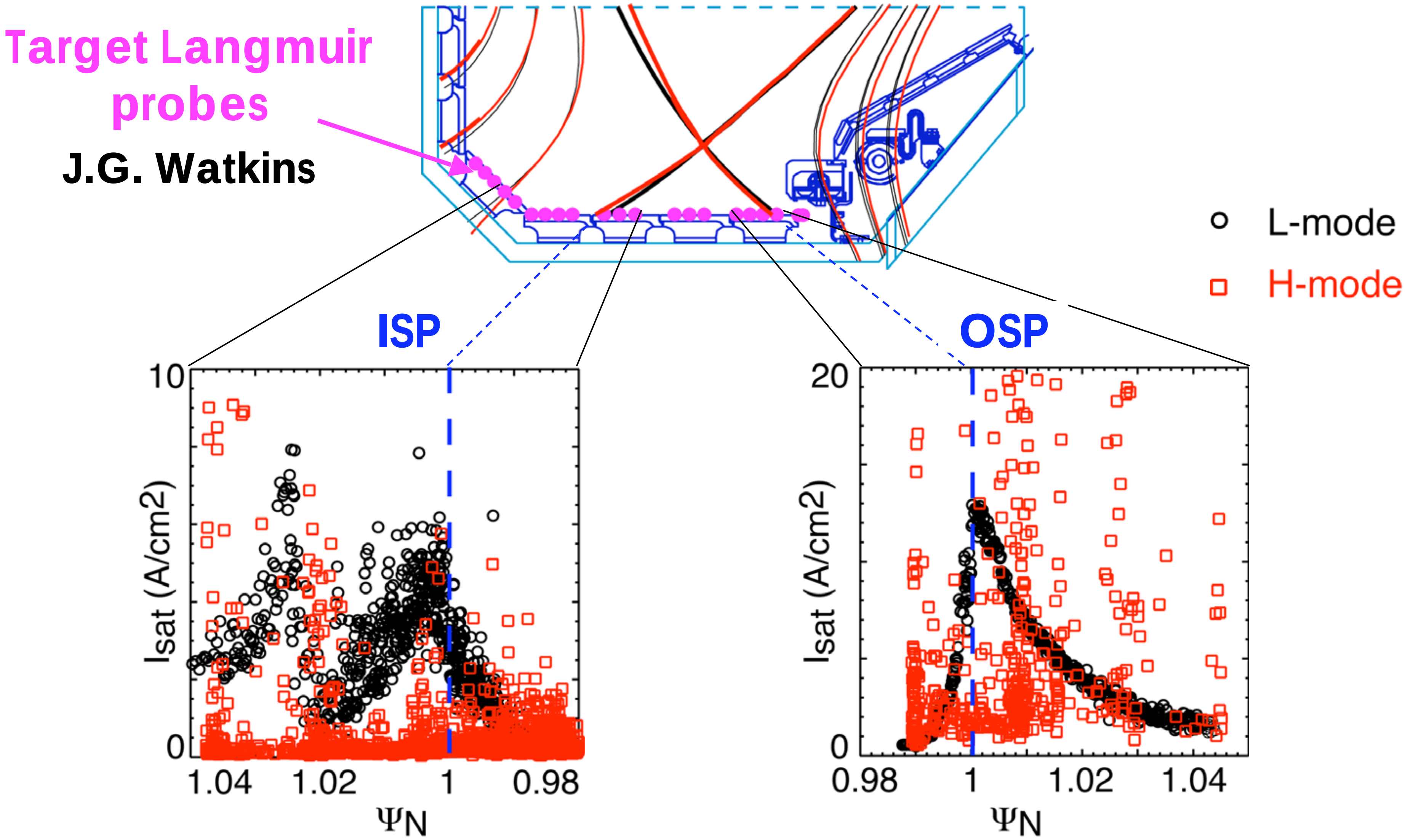

Toroidally Symmetric Injection of $^{13}CH_4$ Had Minimal Effect on the Core Plasma Conditions

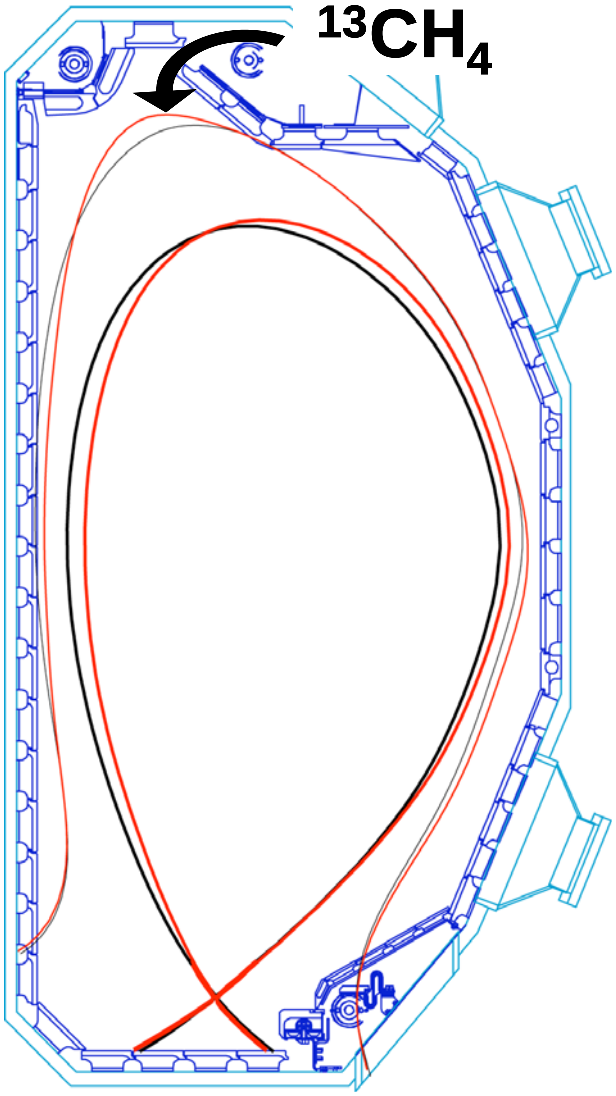

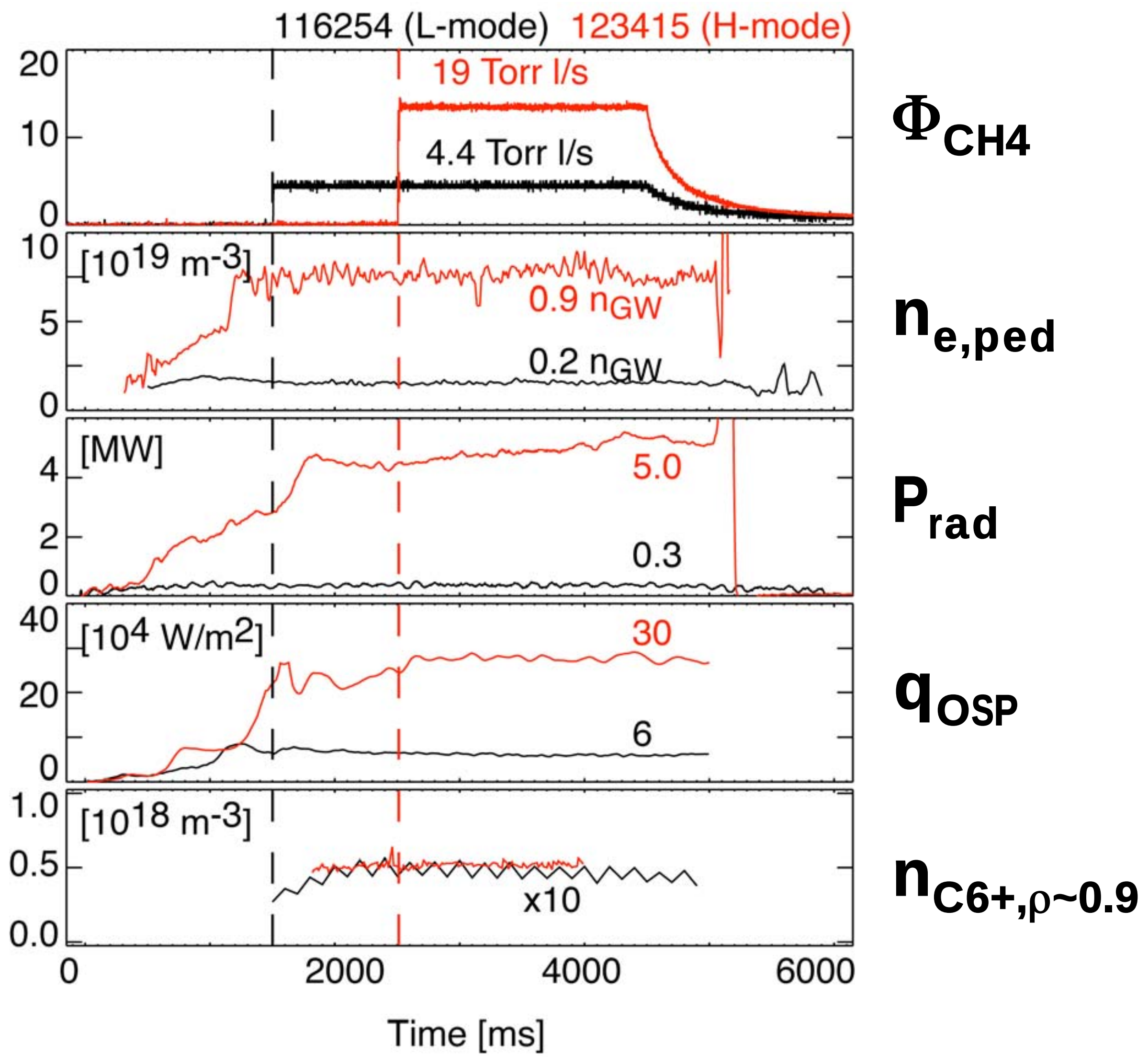

Ex-situ Surface Analysis Measured the Poloidal and Toroidal ^{13}C Surface Density

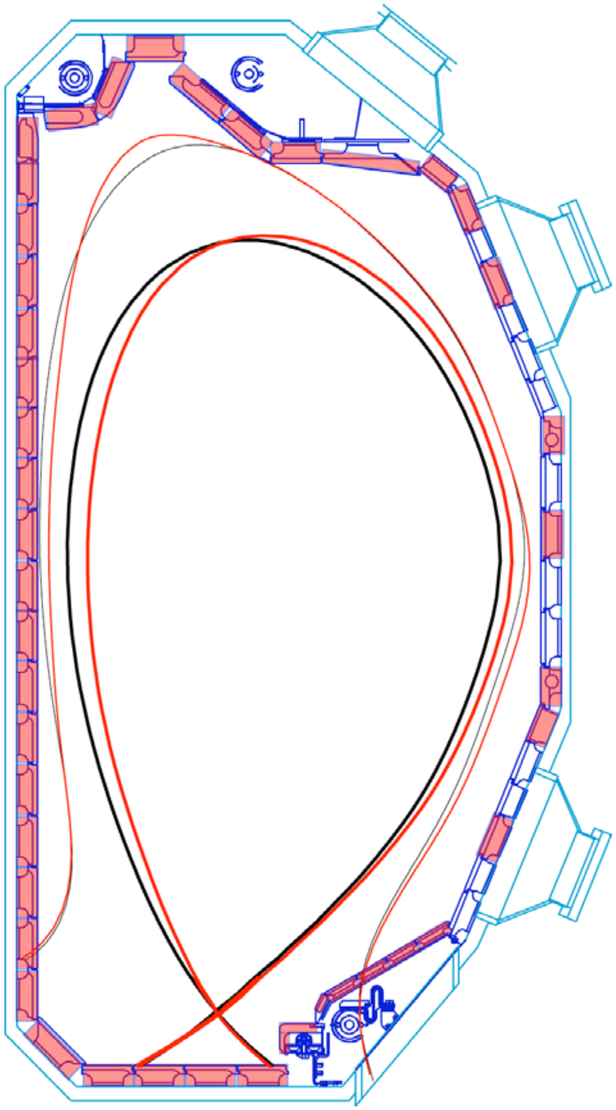

- **Increase ^{13}C surface concentration above natural background by repeating plasma discharges**
  - L-mode: 22 ⇔ 1.0×10^{22} ^{13}C
  - H-mode: 17 ⇔ 2.2×10^{22} ^{13}C
- **Representative set of tiles was removed immediately after venting DIII-D (29/64)**
- **Two methods to measure ^{13}C surface density**
  - Nuclear reaction analysis (SNL: Wampler)
  - Proton-induced γ emission (UWM: Whyte)

Highest Concentration of ^{13}C Deposition Was Measured Along the Divertor Surfaces

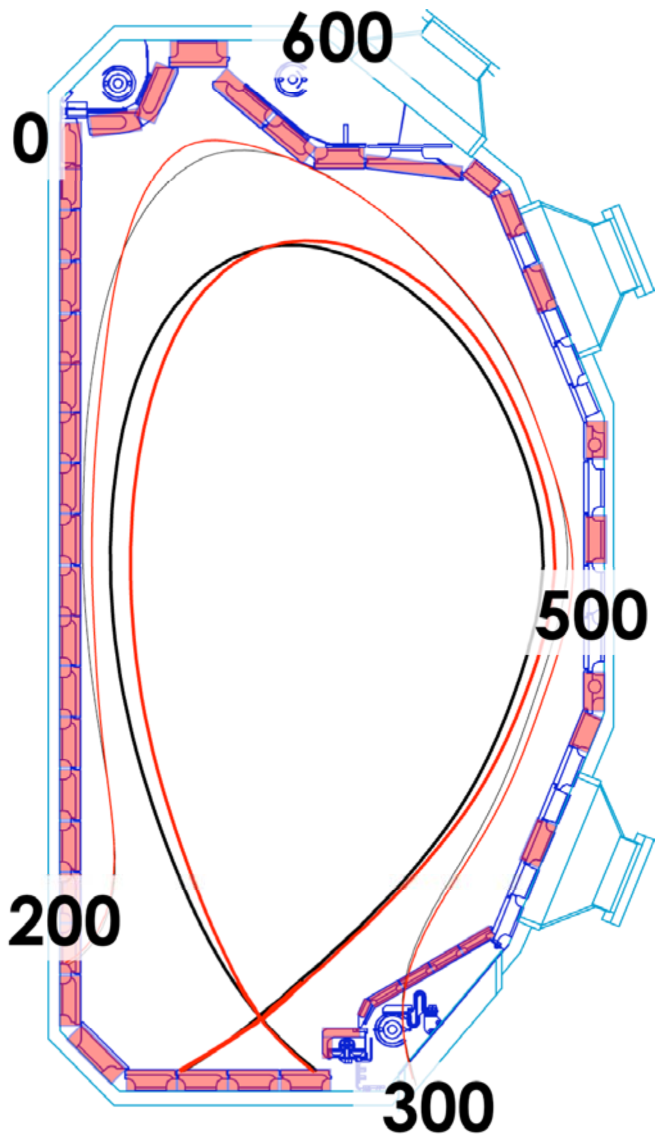

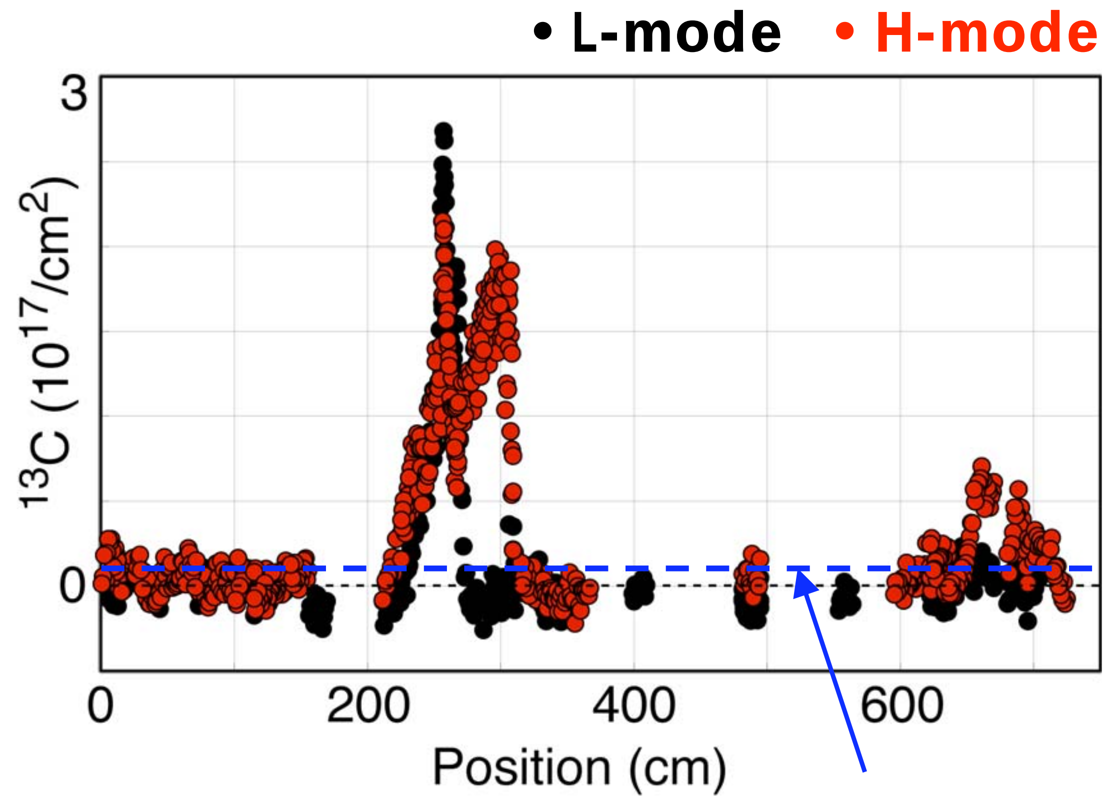

NRA detection limit:
$2x10^{16}$ $^{13}C/cm^2$

Highest Concentration of ^{13}C Deposition Was Measured Along the Divertor Surfaces

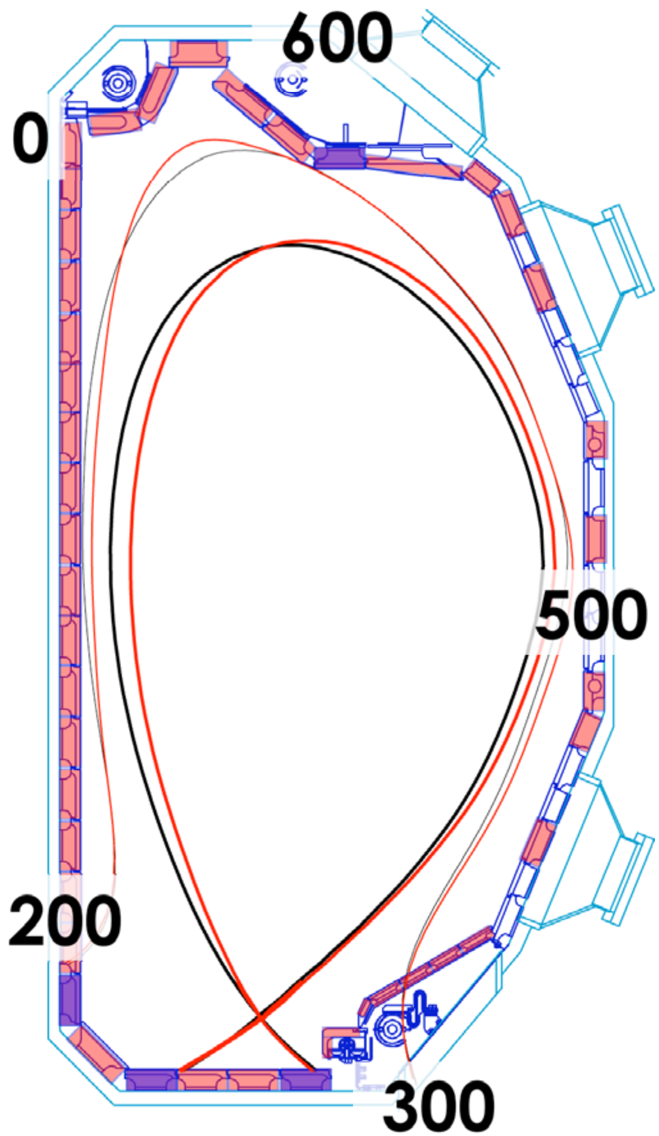

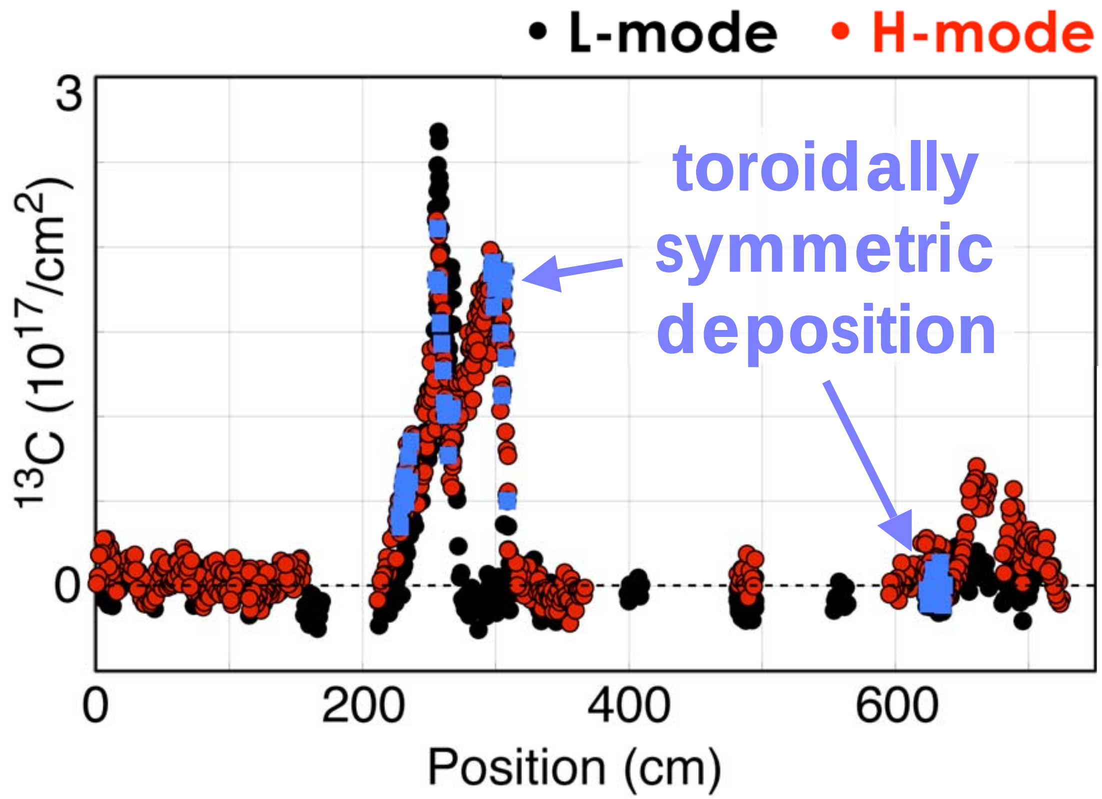

Highest Concentration of ^{13}C Deposition Was Measured Along the Divertor Surfaces

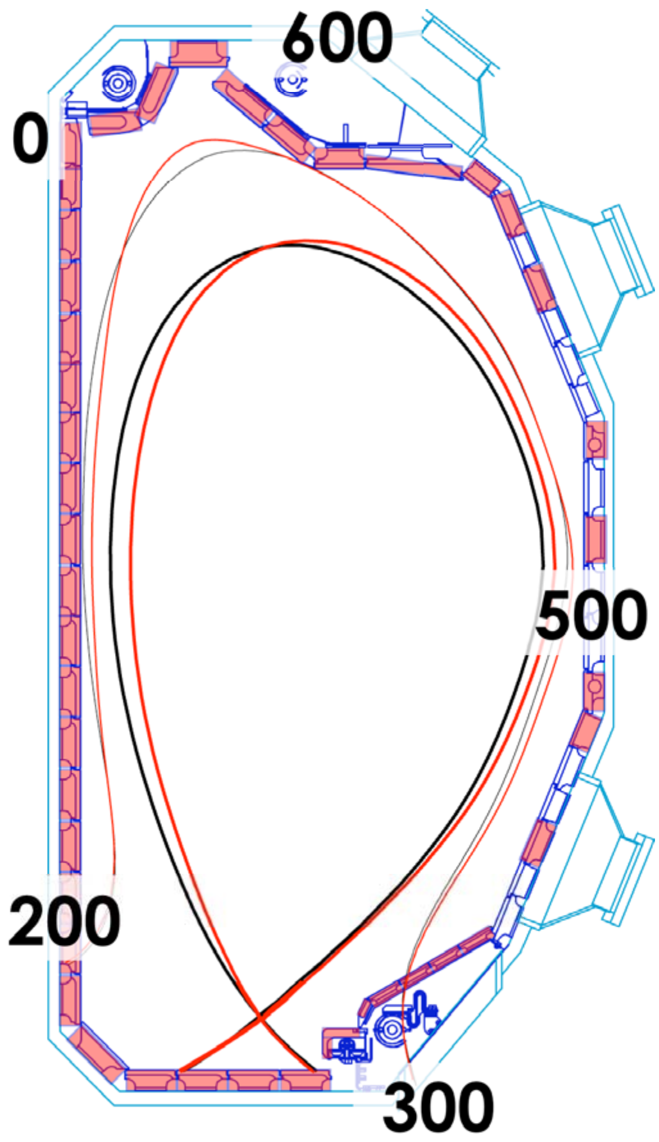

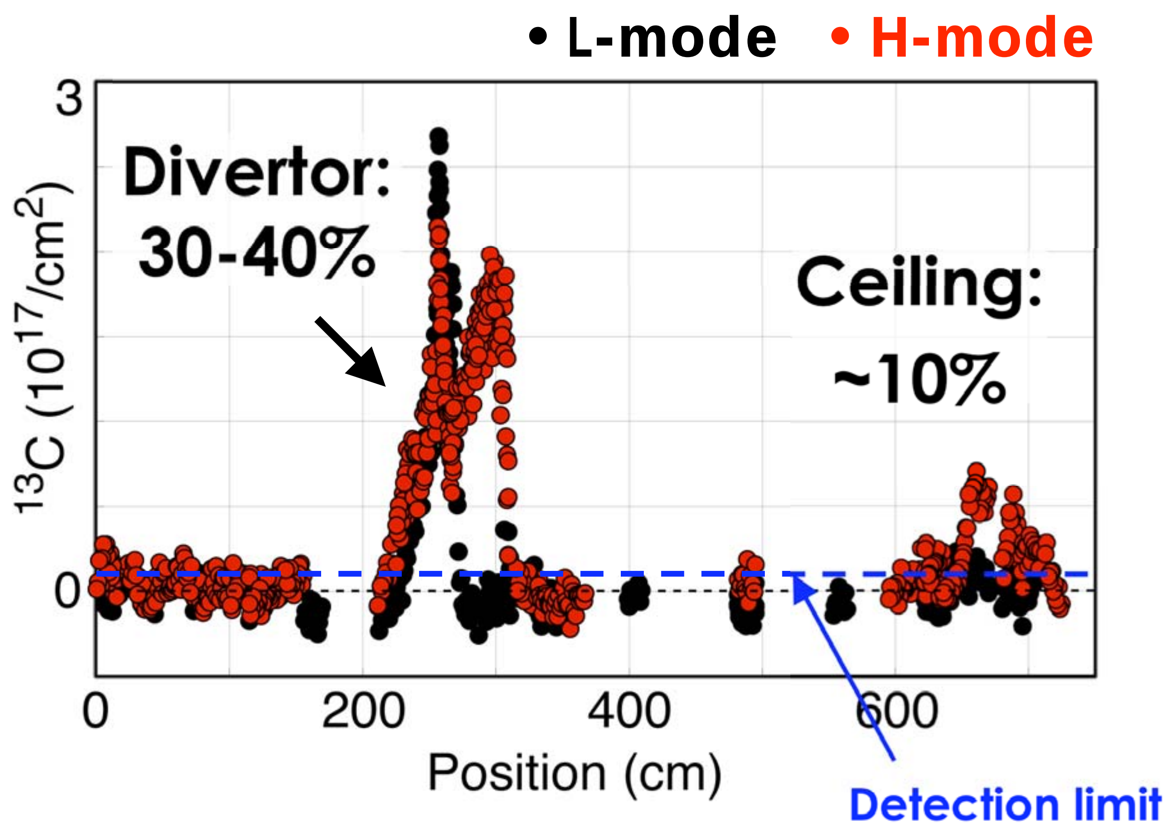

- **PIGE: ~ 30% deposited at low concentration along centerpost**

In L-mode, the ^{13}C Deposition is Peaked at the Corner Formed by Divertor Floor and 45° Angled Divertor Target

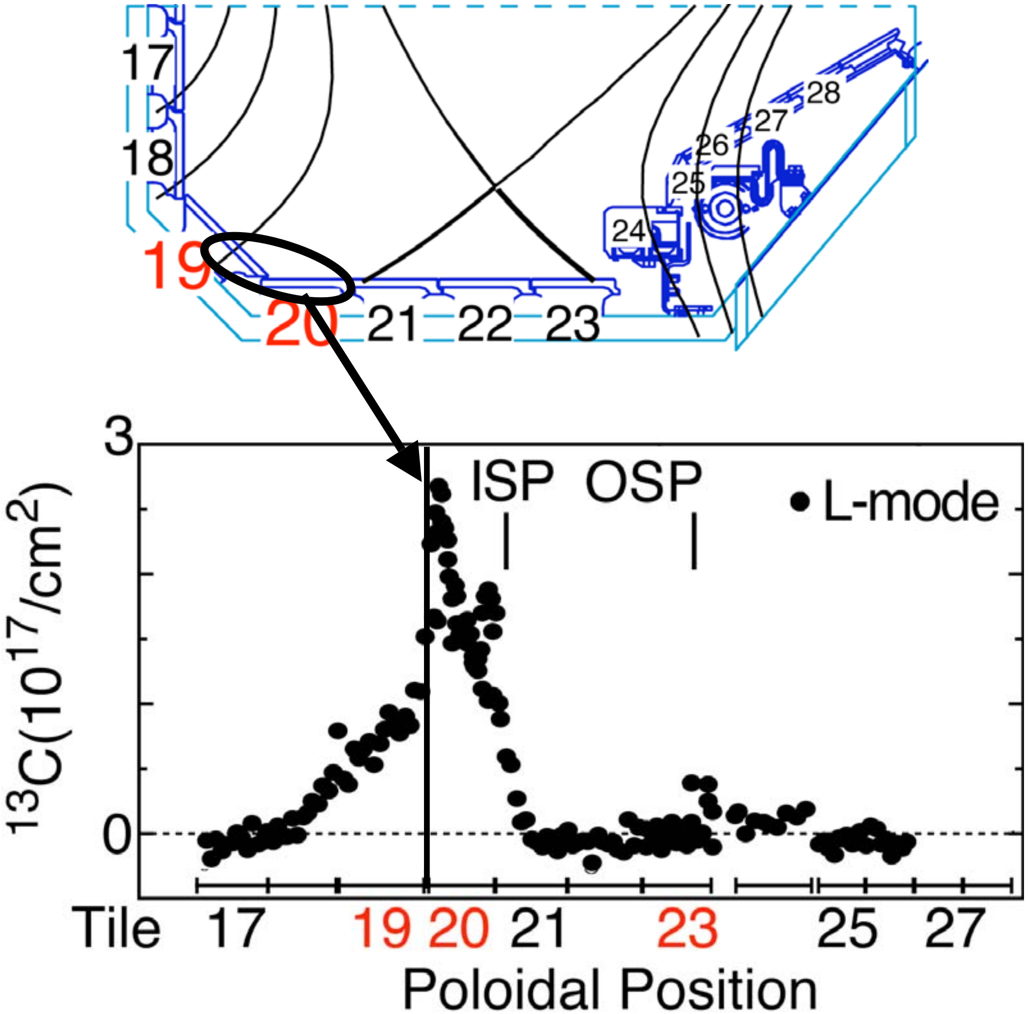

W.R. Wampler

- **Hypothesis: ^{13}C ions injected at the crown enter divertor via inner main SOL**
- **Deposition at the inner plate likely as ions**

In H-mode, Heavy ^{13}C Deposition Was Also Measured Along the Private Flux Surface

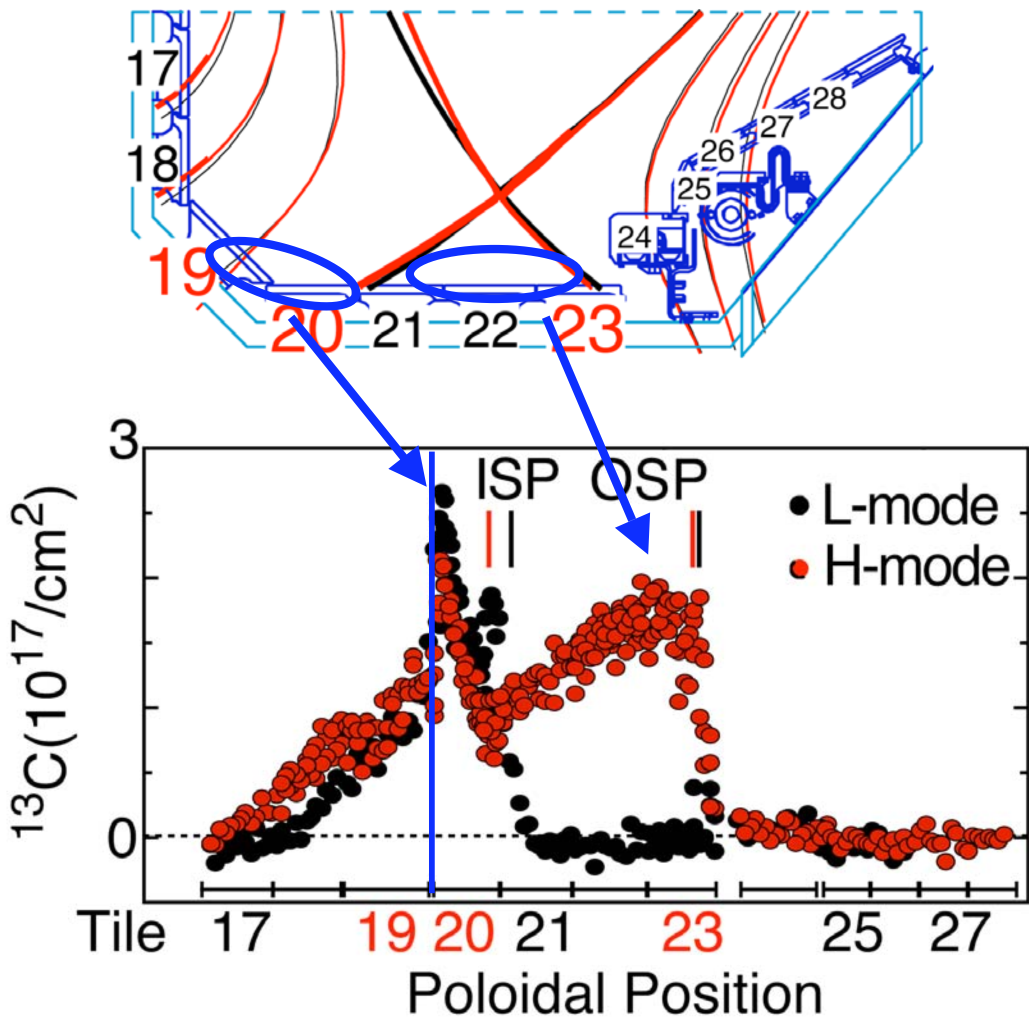

W.R. Wampler

- **Hypothesis: ^{13}C ions injected at the crown enter divertor via inner main SOL**
- **^{13}C ions recombine in cold inner divertor plasma, then deposit as neutrals between ELMs**
- **ELMs may lead to re-erosion of ^{13}C deposits at the inner strike zone**

During ELMs Ionization Front Moved Toward Targets, Which May Lead to Redistribution of the ^{13}C Deposits

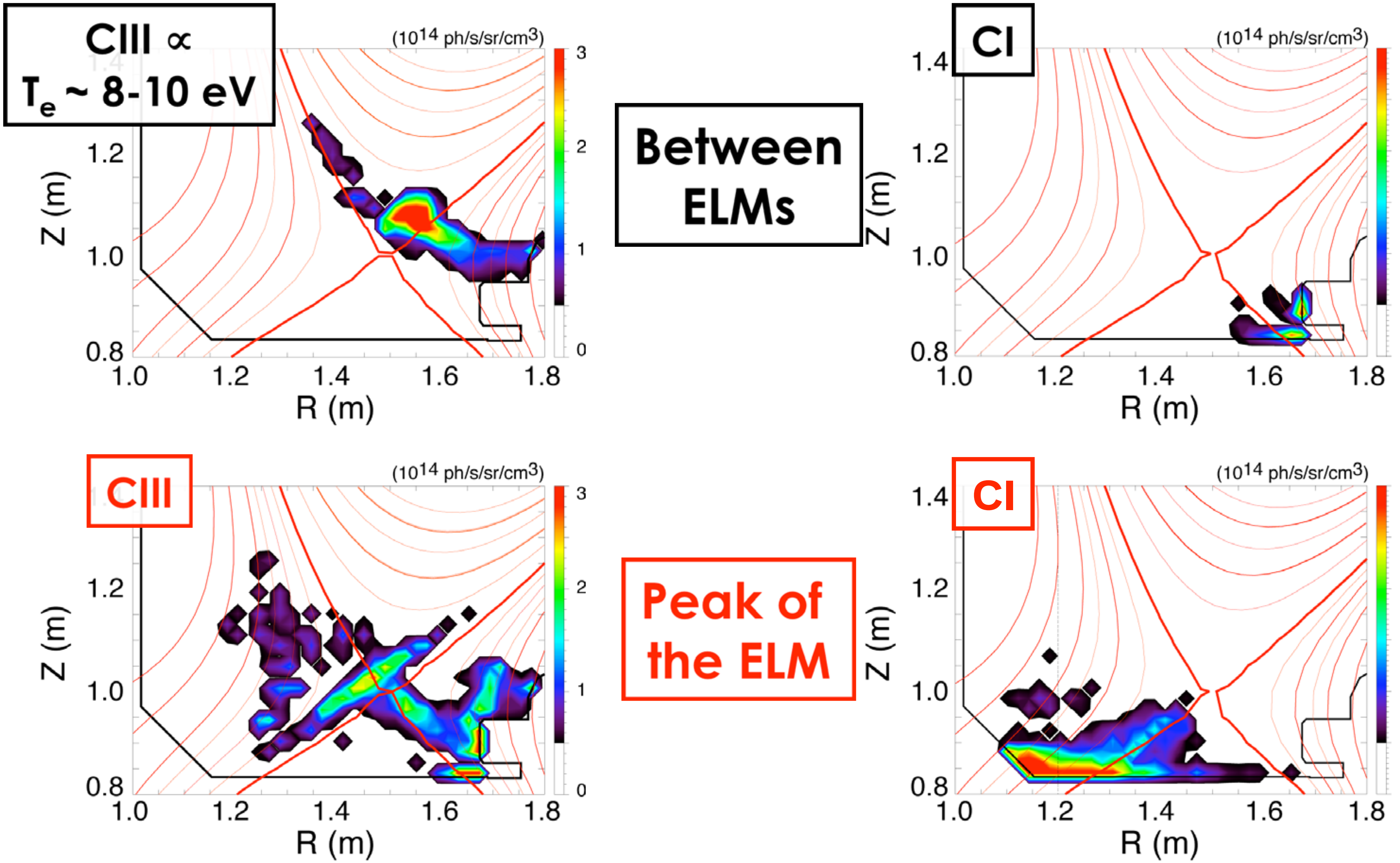

Surface Erosion/Deposition Studies Showed Deuterium and Carbon Deposition in Tile Gaps

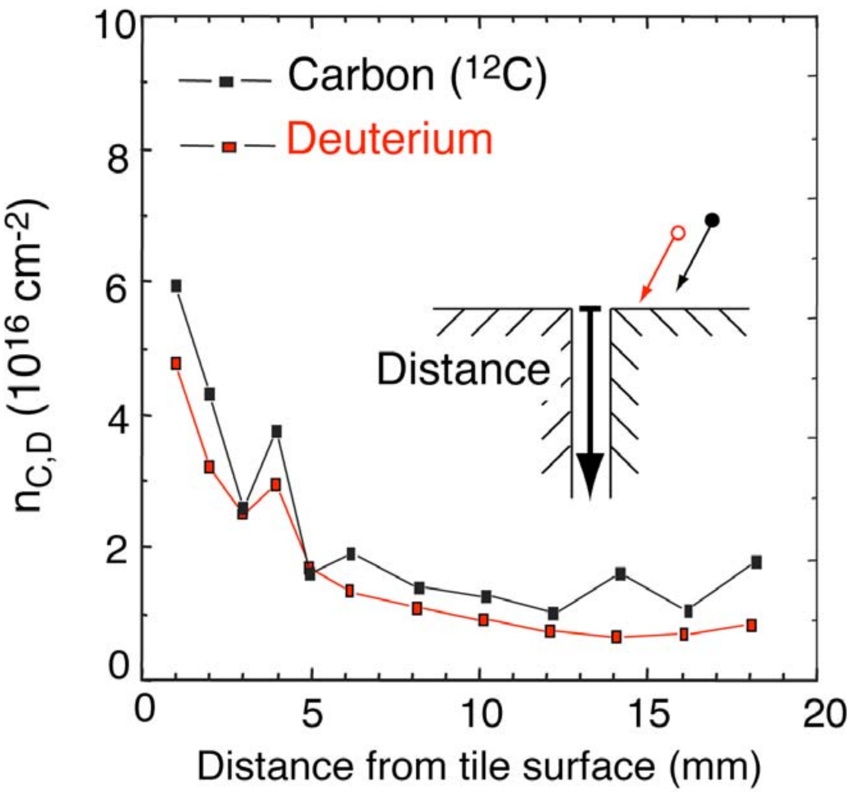

- **^{13}C deposits migrate into plasma-shadowed regions**

⇒ **Long-range migration of ^{13}C into spaces behind tiles yet to be assessed**

- **Deposition process is temperature dependent**
  - Increase of T_{surf} from 30 °C to 200 °C reduced deposition by 3-4x*

*** D.L. Rudakov Phys. Scr. 2006**

W. Jacob, K. Krieger, D.L. Rudakov

Transport and Deposition of Carbon From the Main Chamber Walls Were Investigated in DIII-D by Methane Injection

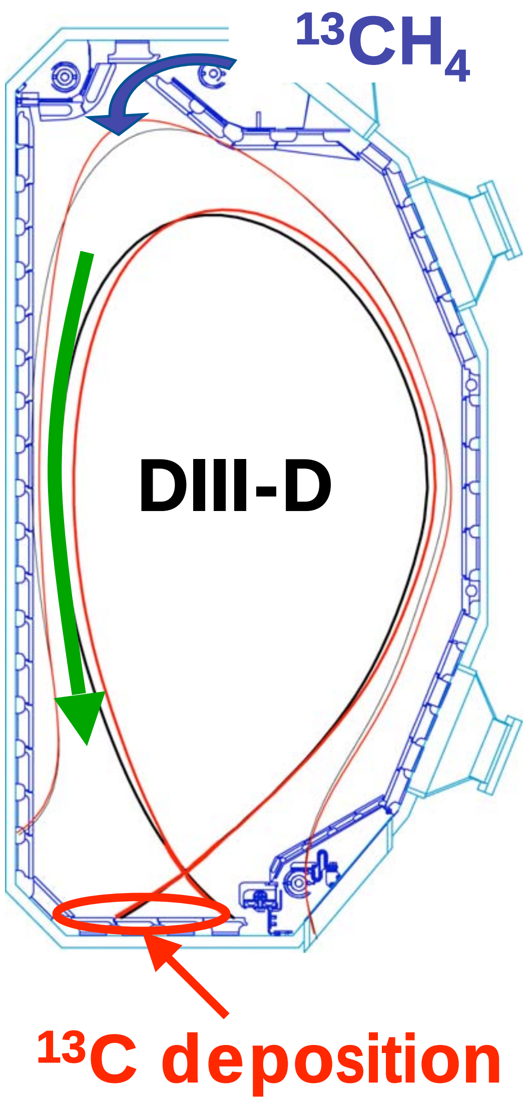

- Toroidally symmetric $^{13}CH_4$ injection into L-mode and H-mode plasmas
- ^{13}C surface analysis: highest ^{13}C concentration along surfaces exposed to cold divertor plasmas
- **Carbon transport from the crown to the inner divertor via frictional coupling to deuteron flow**
- Carbon transport and deposition simulations

CH_4 Breakup Followed by Imaging of the Emission From C-H Radical in the Plasma Crown

L-mode

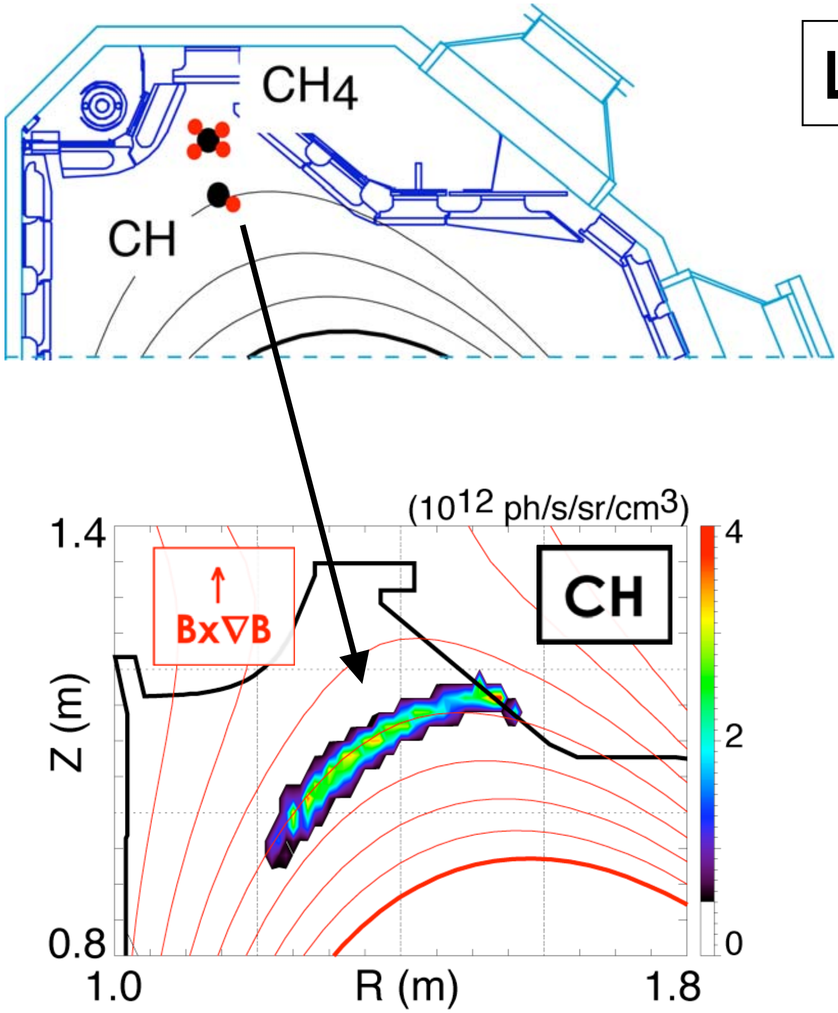

Emission From Low Charge State Carbon Ions Suggests Carbon Transport Toward Inner Divertor

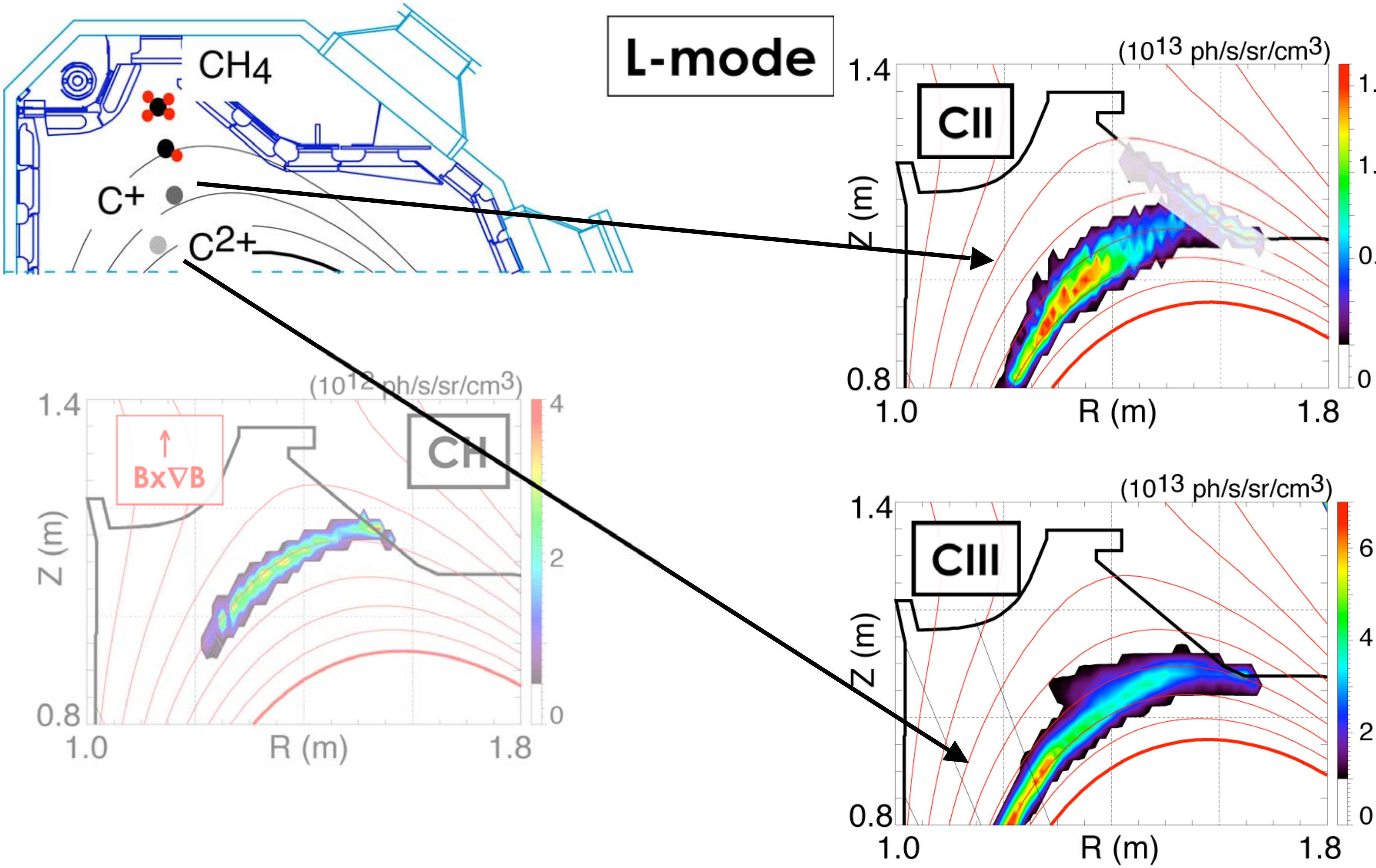

Maximum C^+ Ion Velocity Along the Field Line is 15 km s^{-1}

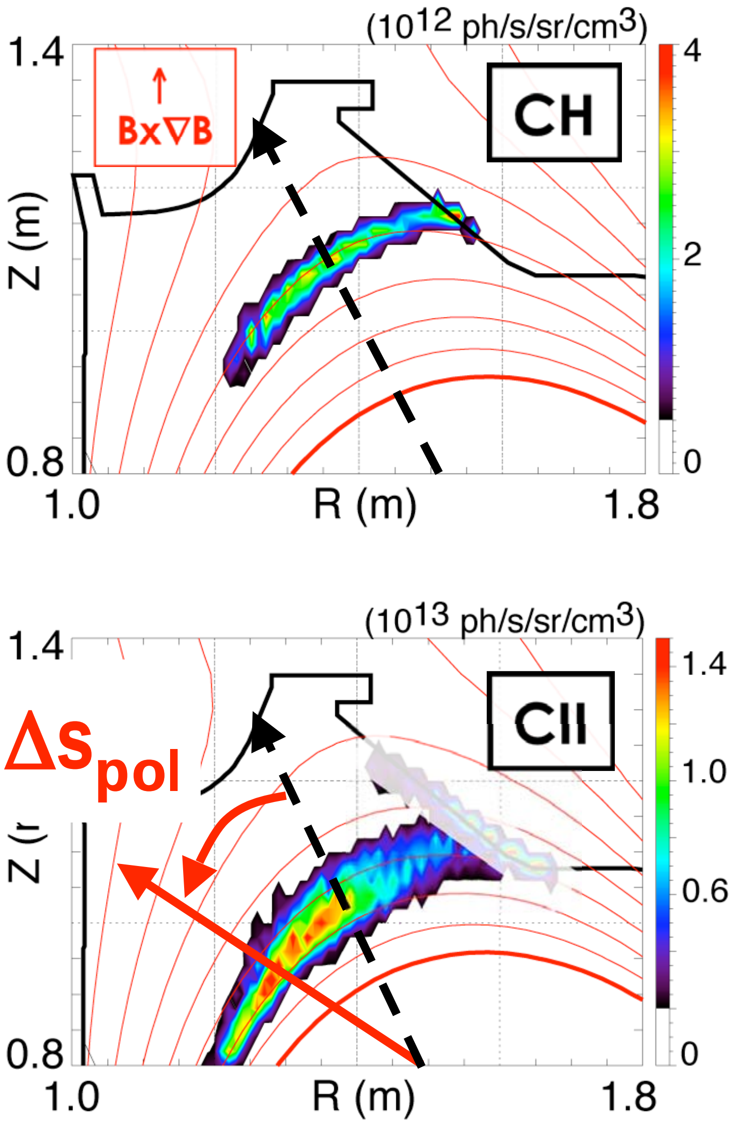

L-mode

$$v_{\parallel}^{C^+} \leq \frac{B}{B_{pol}} \frac{\Delta s_{pol}}{t_{ioniz}^{C^+ \to C^{2+}}}$$

Carbon Ions Are Entrained in the Deuteron SOL Flow of $M_{||}$ ~0.5 Via Frictional Coupling

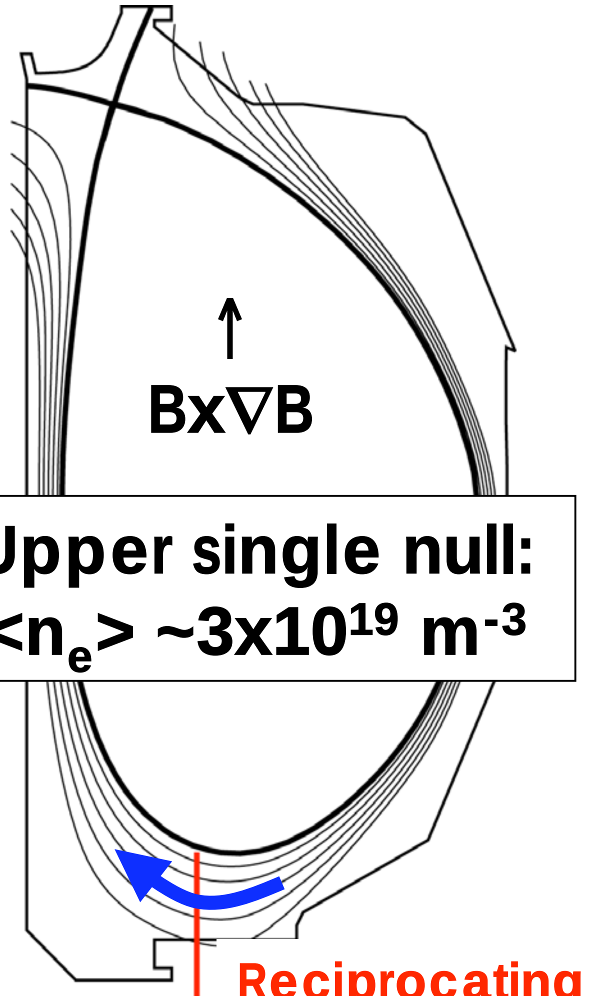

Upper single null:
$\langle n_e \rangle$ ~3×10^{19} m^{-3}

L-mode

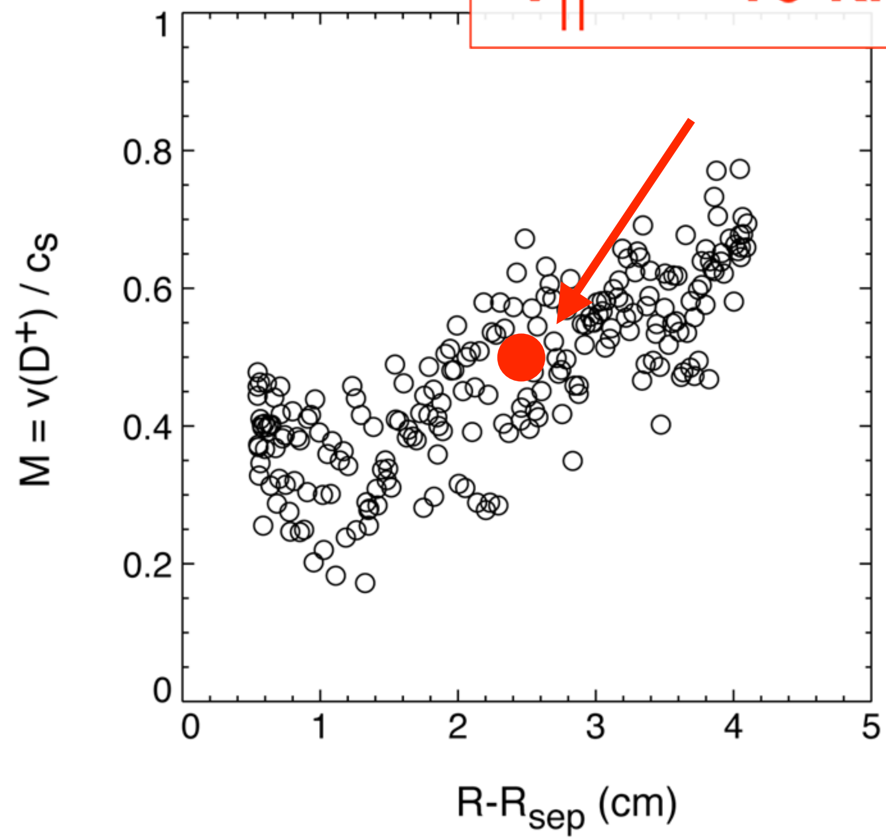

T_e ~ 10 eV:
$V_{||}^{D+}$ ~ 15 km s^{-1}

Inner target

J.A. Boedo

Increase in CIII Emission at the Inner Midplane With $^{13}CH_4$ Injection Indicates Carbon Flow Continues Toward Inner Plate

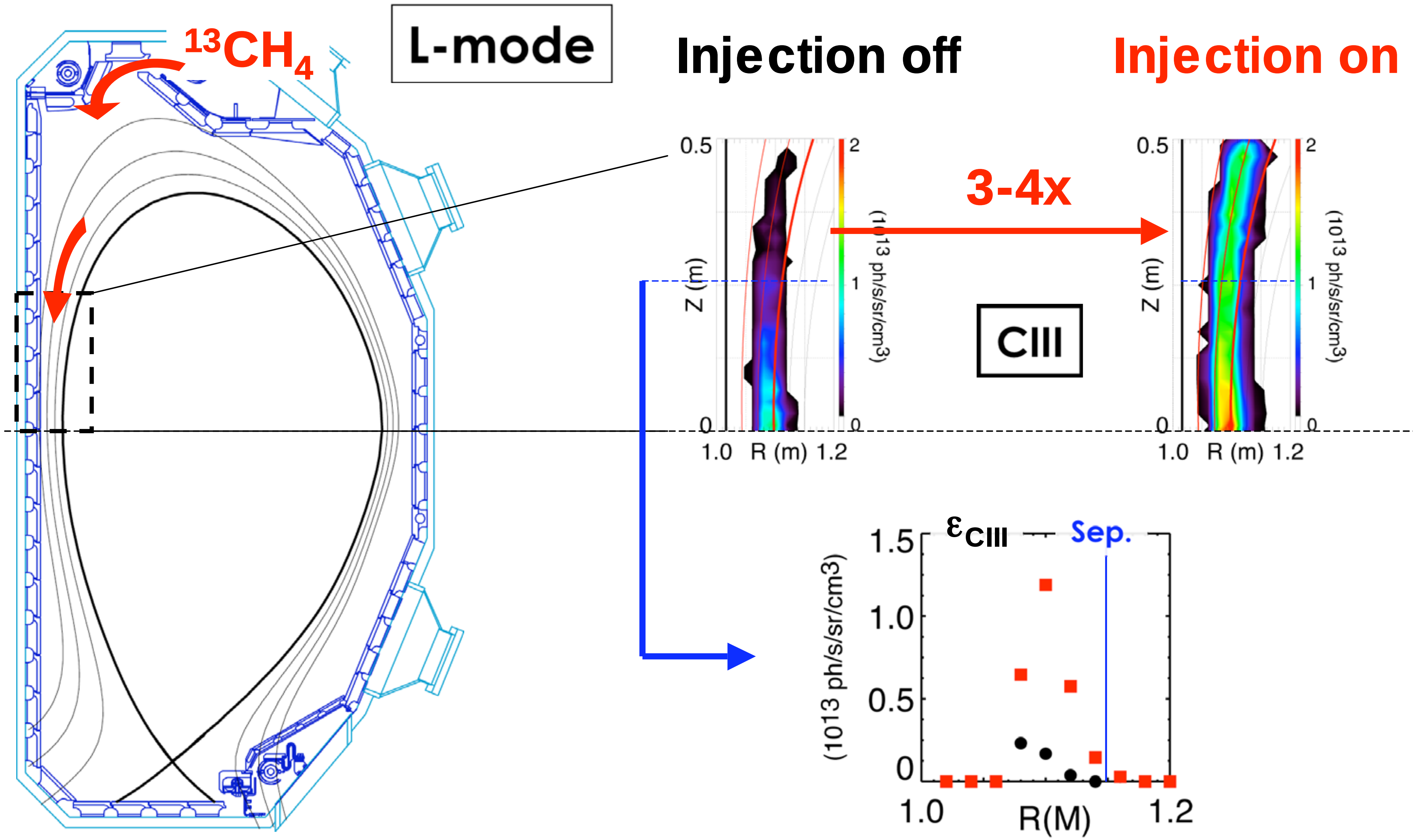

In H-mode, Penetration of Methane is Significantly Shallower

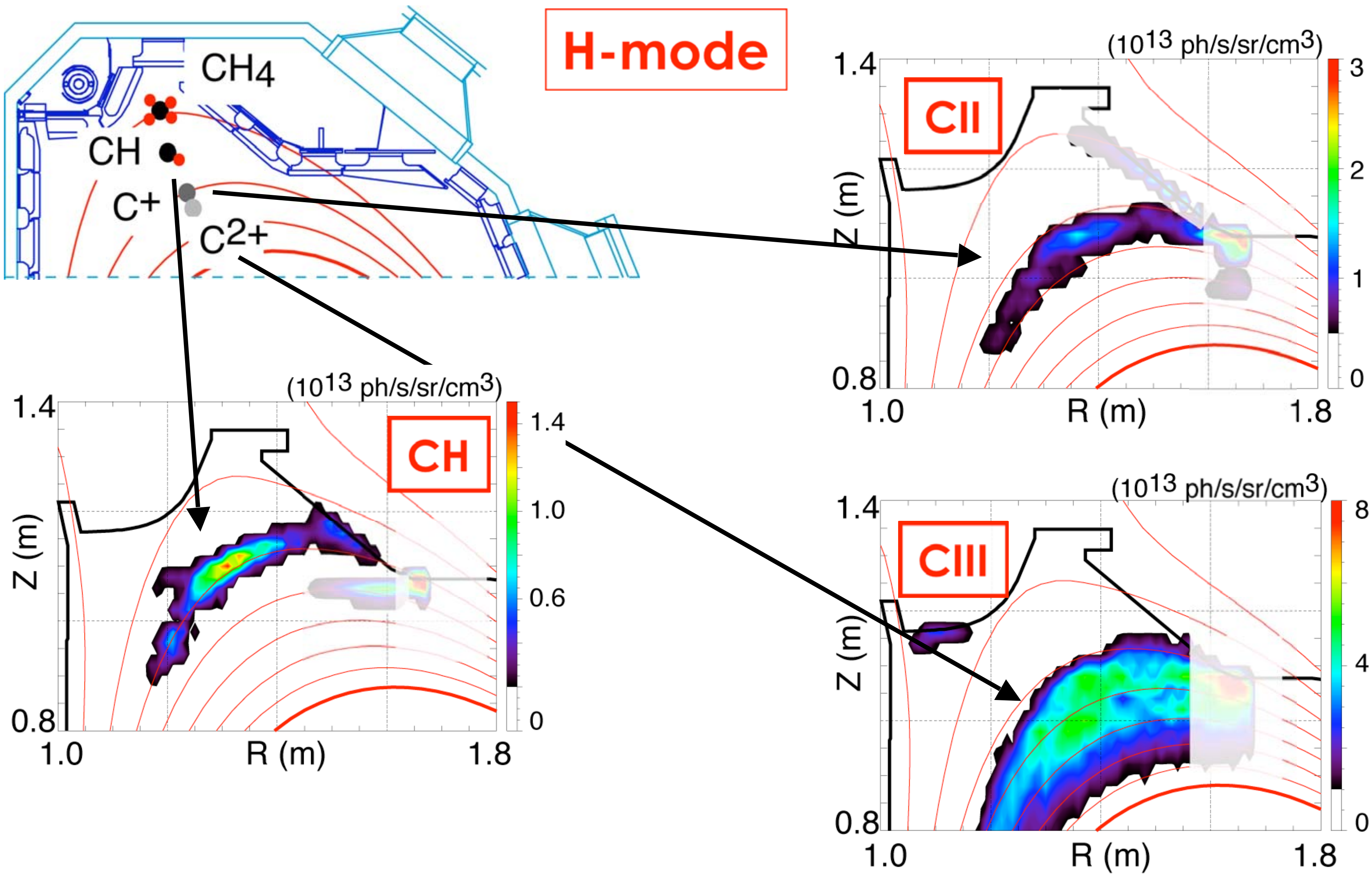

Imaging of the Carbon Emission From the Crown Did Not Indicate Carbon Flow Toward Inner Target

H-mode

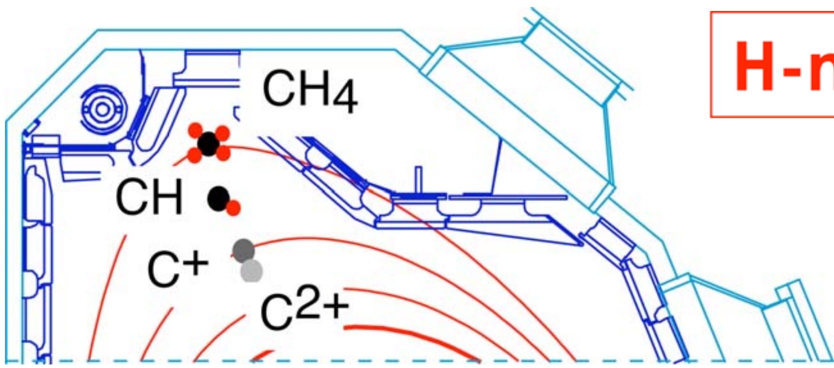

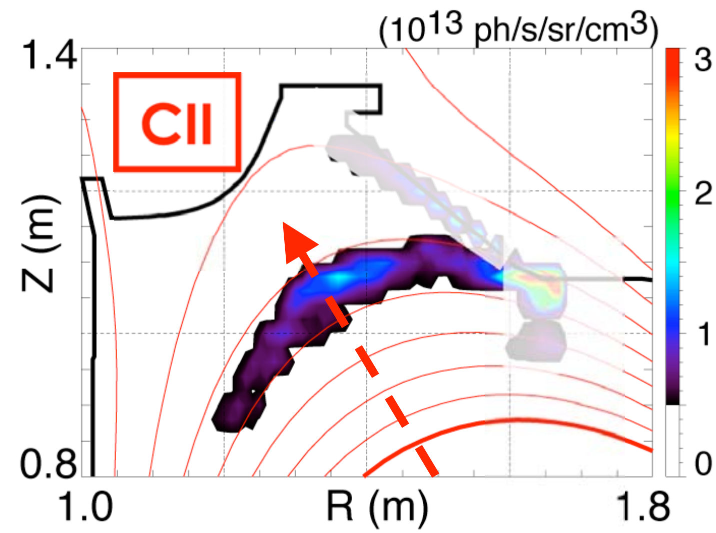

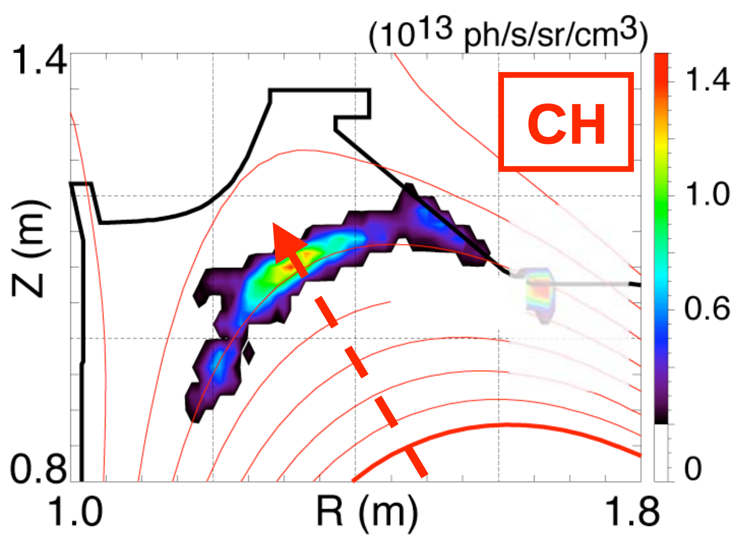

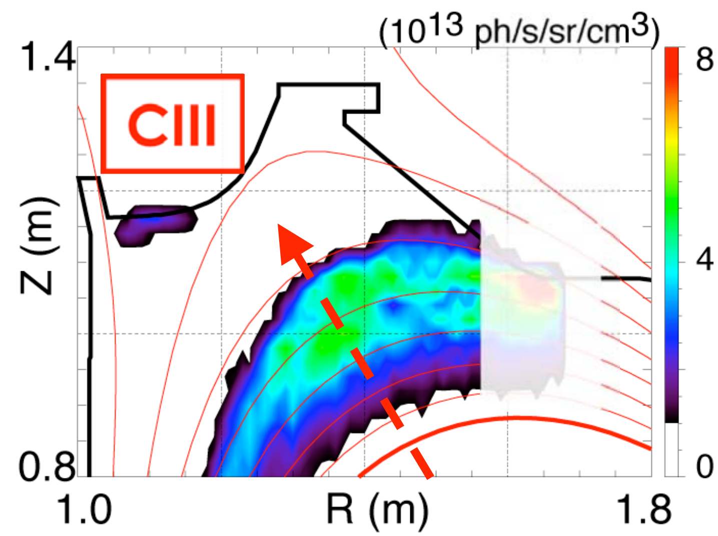

Increase in CIII Emission at the Inner Midplane With $^{13}CH_4$ Injection, However, Indicates Carbon Flow Toward Inner Plate

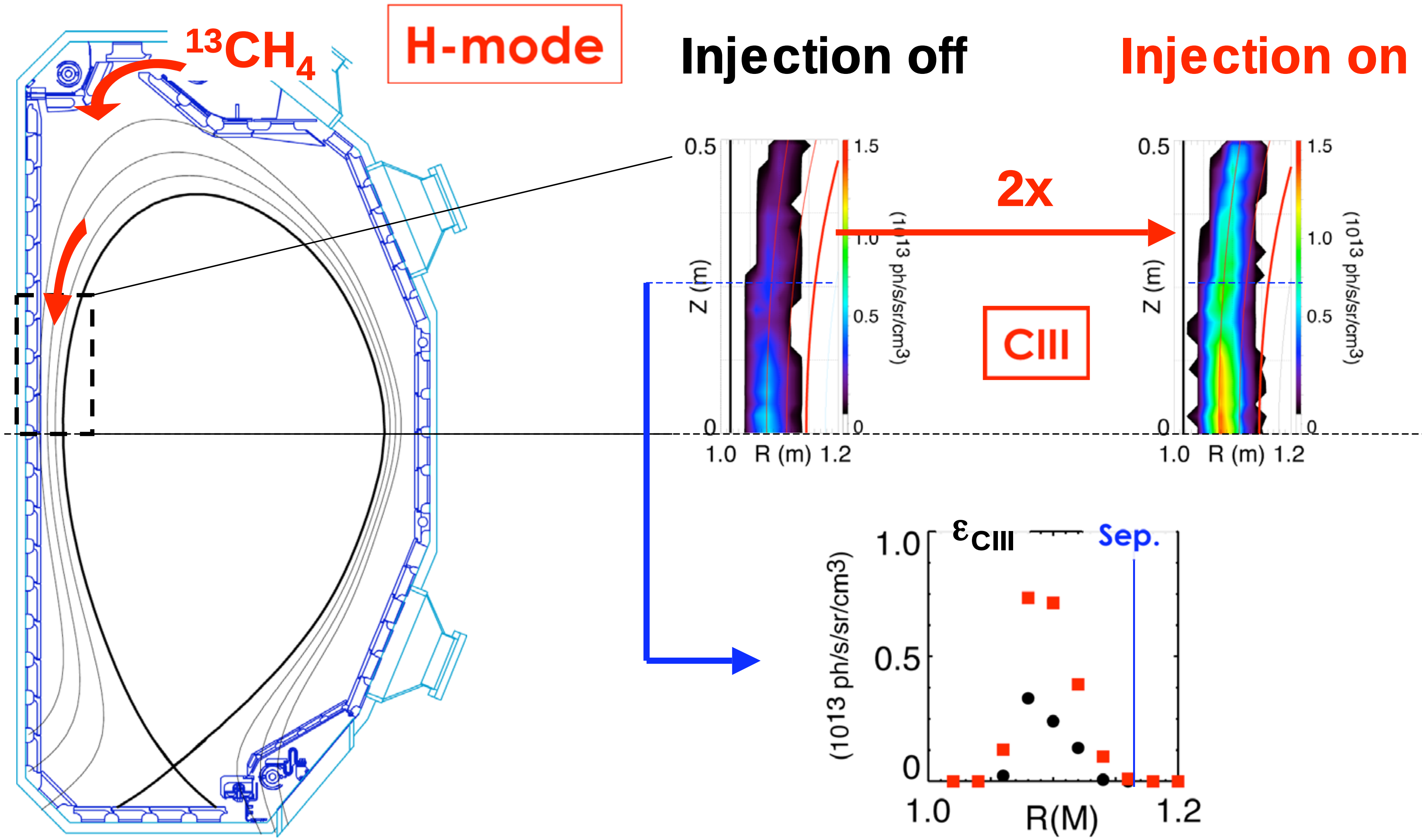

Transport and Deposition of Carbon From the Main Chamber Walls Were Investigated in DIII-D by Methane Injection

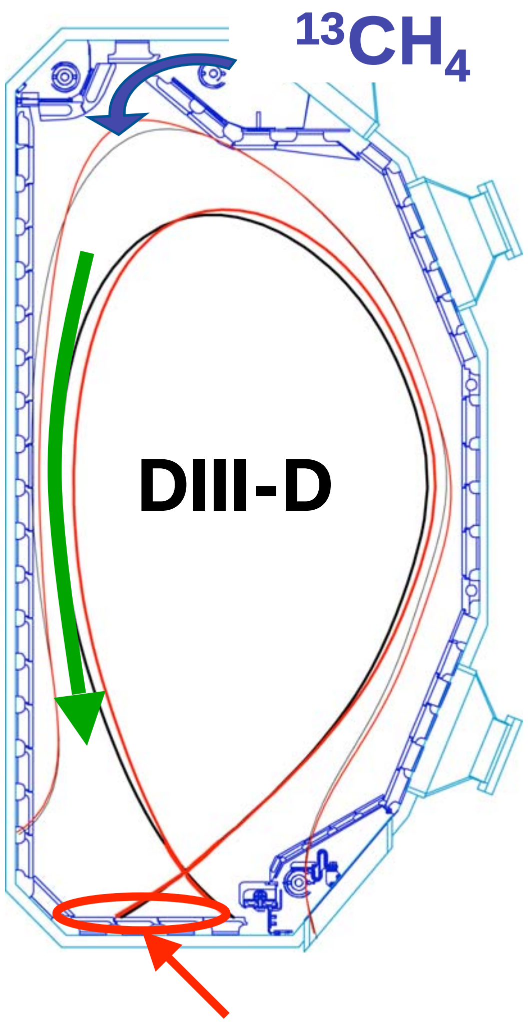

- Toroidally symmetric $^{13}CH_4$ injection into L-mode and H-mode plasmas
- ^{13}C surface analysis: highest ^{13}C concentration along surfaces exposed to cold divertor plasmas
- Carbon transport from the crown to the inner divertor via frictional coupling to deuteron flow
- **Carbon transport and deposition simulations**

^{13}C Transport and Deposition Simulations Were Carried Out With the Oedge/Hydrocarbon (HC) and UEDGE Codes

Boundary plasma simulations

- **Interpretative OEDGE/ hydrocarbon model**
  - Prescribed background plasma from experiment
  - Ad-hoc parallel and radial flows
  - Model of CH_4 dissociative breakup and ionization

- **'Predictive' UEDGE model**
  - Background plasma calculated from first-principle fluid flow physics, and assumed radial transport model
  - Intrinsic carbon
  - Flows are self-consistently calculated from ionization balance and drifts

^{13}C Transport and Deposition Simulations Were Carried Out With the Oedge/Hydrocarbon (HC) and UEDGE Codes

Boundary plasma simulations

- **Interpretative OEDGE/ hydrocarbon model**
  - Prescribed background plasma from experiment
  - Ad-hoc parallel and radial flows
  - Model of CH_4 dissociative breakup and ionization

- **'Predictive' UEDGE model**
  - Background plasma calculated from first-principle fluid flow physics, and assumed radial transport model
  - Intrinsic carbon
  - Flows are self-consistently calculated from ionization balance and drifts

Interpretative Modeling With OEDGE/HC Uses Ad-hoc Flow of Carbon Ions to Match Measured CIII Emission Profiles

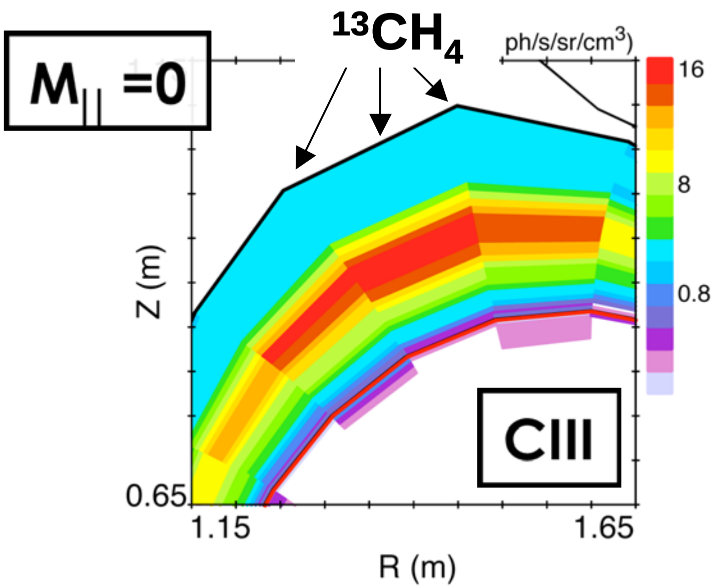

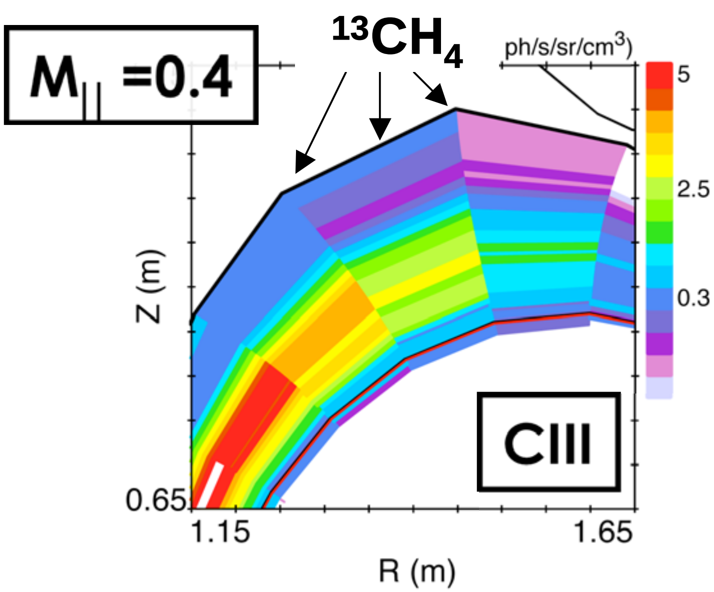

L-mode

- **Hydrocarbon physics model and carbon ion diffusion produce radial profiles consistent with the measured CII and CIII emission**
- **Poloidal shift of CIII emission achieved by imposing carbon flow velocity of 10-15 km s^{-1}, consistent with measurements**

J.D. Elder
A.G McLean

Inward SOL Pinch Was Used to Match Measured ^{13}C Deposition Profile Assuming First Deposition

L-mode

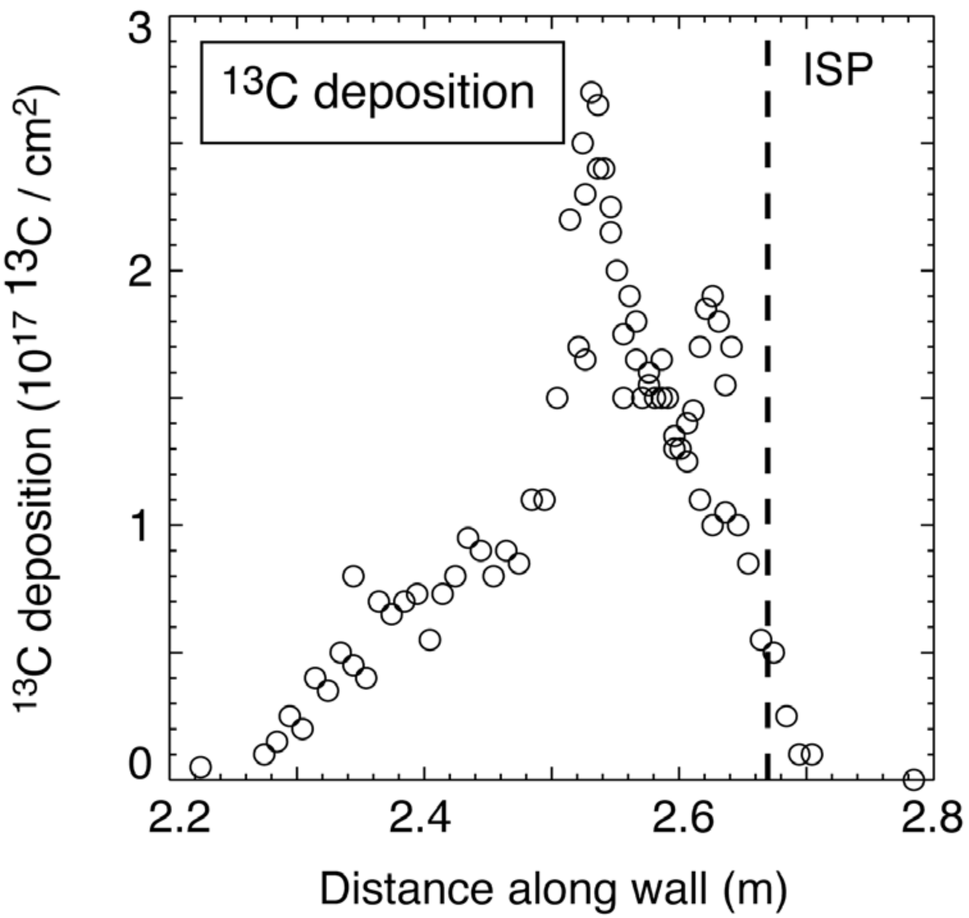

J.D. Elder

Inward SOL Pinch Was Used to Match Measured ^{13}C Deposition Profile Assuming First Deposition

L-mode

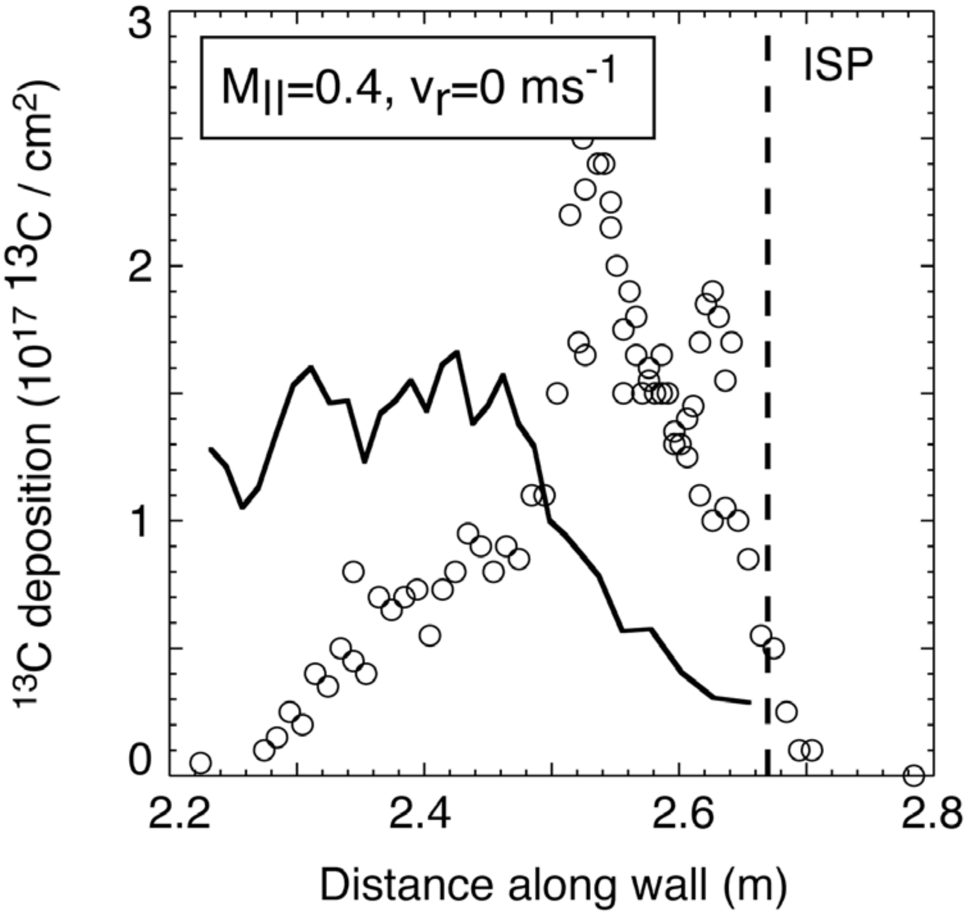

- **OEDGE ad-hoc parallel transport leads to ^{13}C deposition in far SOL only**

J.D. Elder

Inward SOL Pinch Was Used to Match Measured ^{13}C Deposition Profile Assuming First Deposition

L-mode

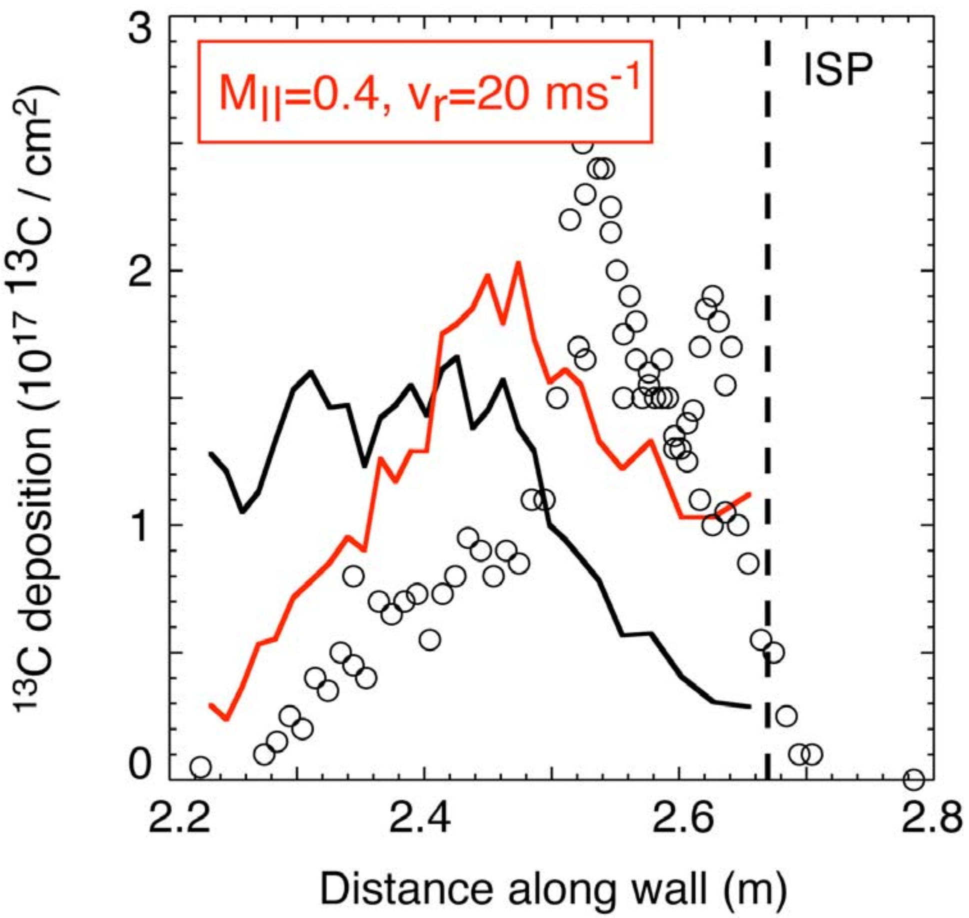

- **OEDGE ad-hoc parallel transport leads to ^{13}C deposition in far SOL only**

⇒ **Apply additional radial pinch (nv_r) to move ^{13}C ions closer to separatrix**

J.D. Elder

Inward SOL Pinch Was Used to Match Measured ^{13}C Deposition Profile Assuming First Deposition

L-mode

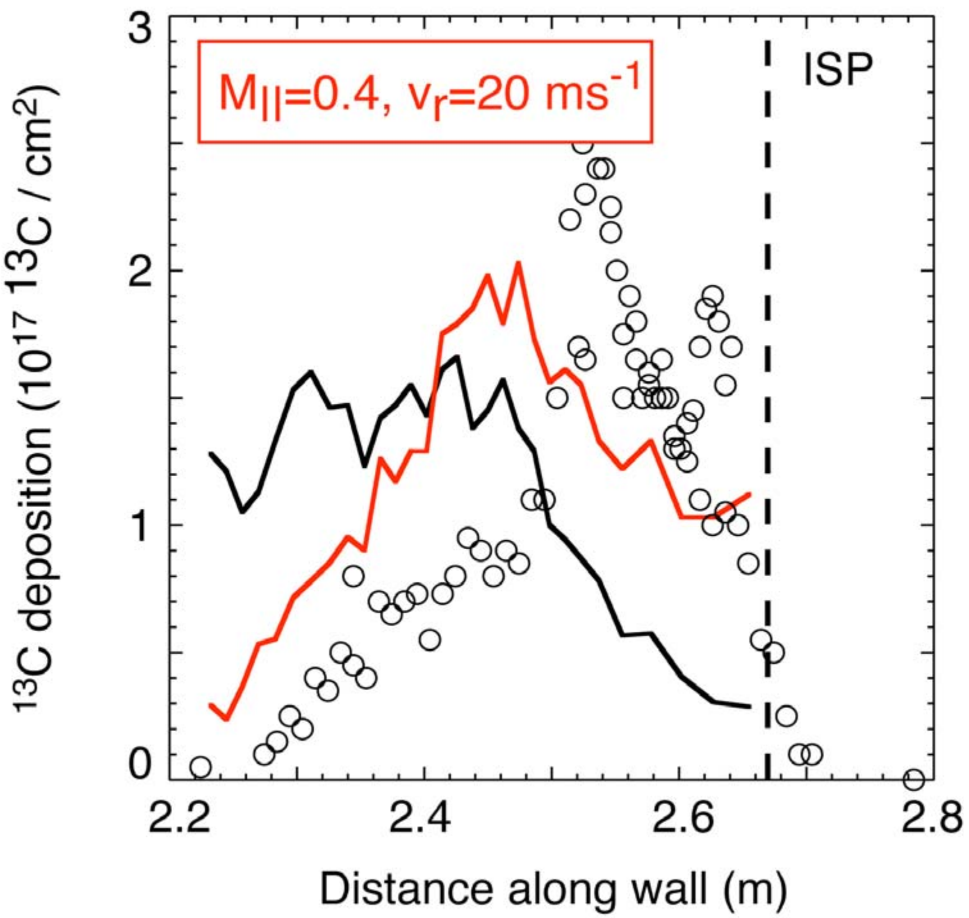

- **OEDGE ad-hoc parallel transport leads to ^{13}C deposition in far SOL only**

⇒ **Apply additional radial pinch (nv_r) to move ^{13}C ions closer to separatrix**

- **H-mode data may also be modeled by combination of parallel and radial transport (including ELMs)**

J.D. Elder

^{13}C Transport and Deposition Simulations Were Carried Out With the Oedge/Hydrocarbon (HC) and UEDGE Codes

Boundary plasma simulations

- **Interpretative OEDGE/ hydrocarbon model**
  - Prescribed background plasma from experiment
  - Ad-hoc parallel and radial flows
  - Model of CH_4 dissociative breakup and ionization

- **'Predictive' UEDGE model**
  - Background plasma calculated from first-principle fluid flow physics, and assumed radial transport model
  - Intrinsic carbon
  - Flows are self-consistently calculated from ionization balance and drifts

UEDGE Reproduces Multiple Diagnostics in the Divertor and Main Chamber SOL Simultaneously

L-mode

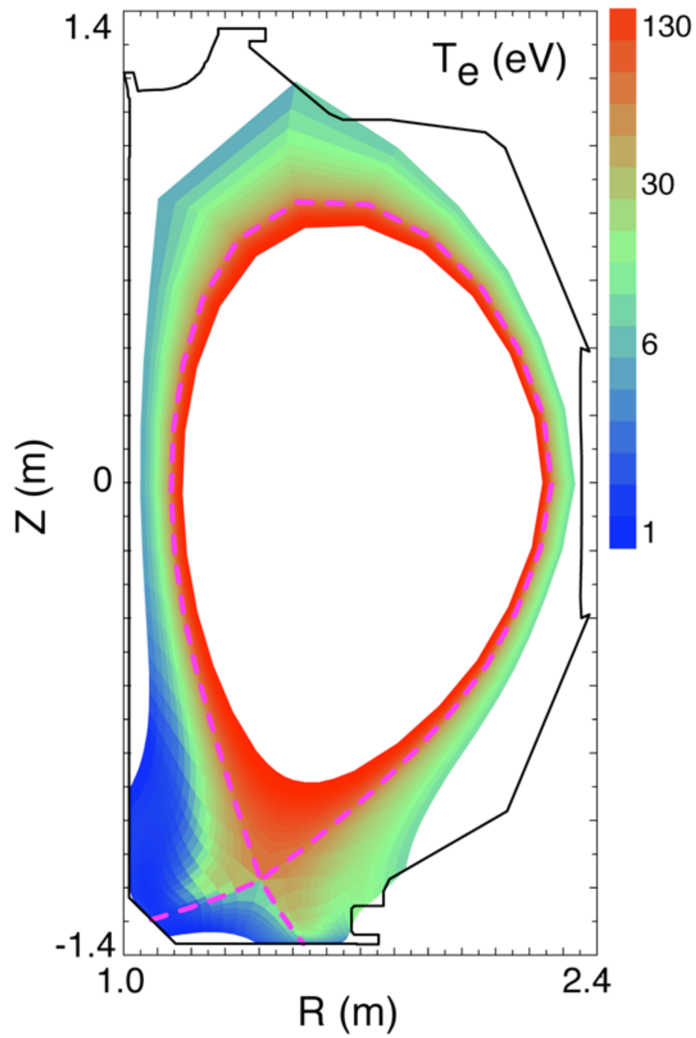

- **UEDGE predicts $T_{e,ISP}$ ~ 1.5 eV, consistent with measurements in inner divertor**
  - Inner strike point D_β/D_α ~ 0.15
  - Lack of CII emission in the inner leg

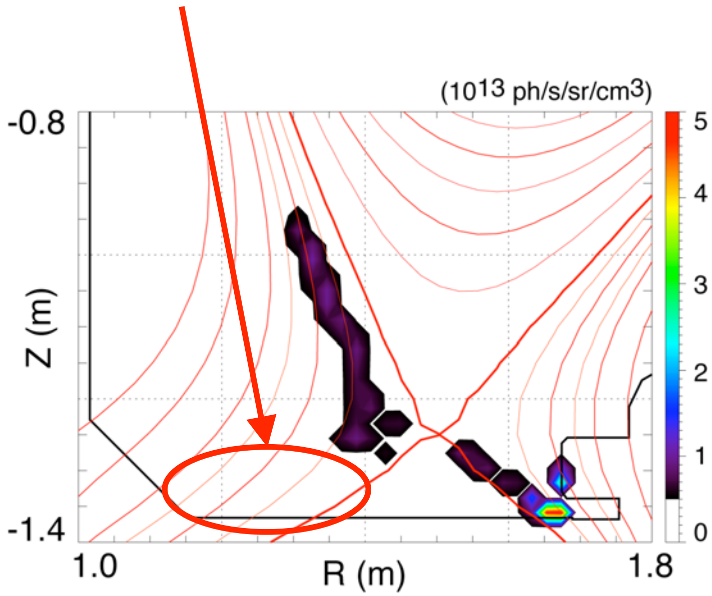

UEDGE Reproduces Multiple Diagnostics in the Divertor and Main Chamber SOL Simultaneously

L-mode

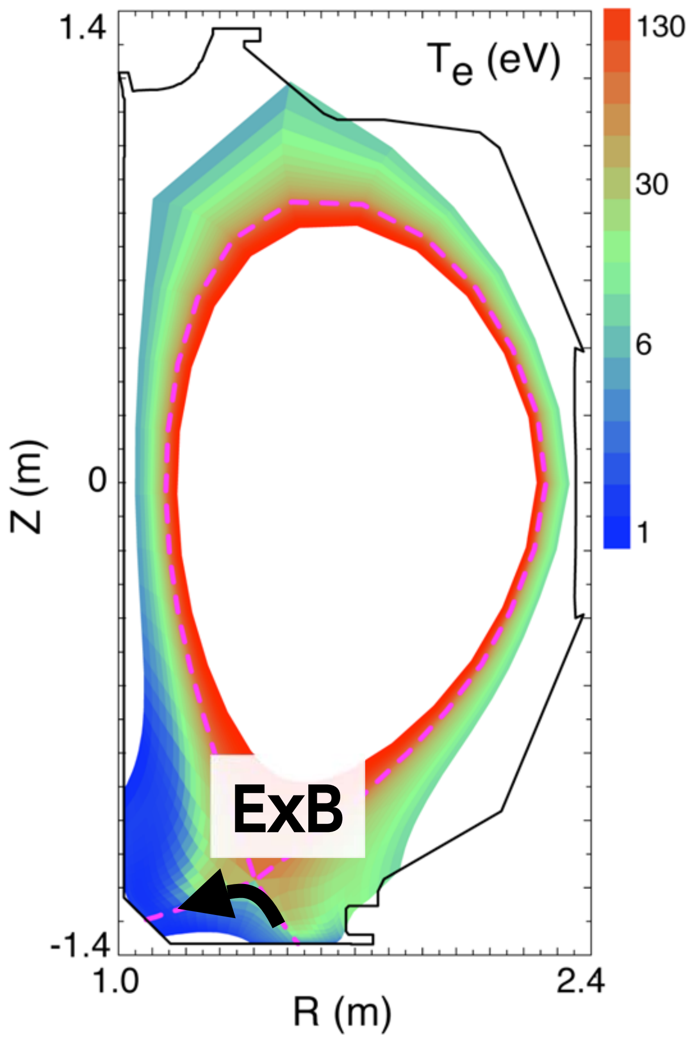

- **UEDGE predicts $T_{e,ISP}$ ~ 1.5 eV, consistent with measurements in inner divertor**
  - Inner strike point D_β/D_α ~ 0.15
  - Lack of CII emission in the inner leg
- **ExB drifts play an important role in obtaining low $T_{e,ISP}$**

UEDGE Reproduces Multiple Diagnostics in the Divertor and Main Chamber SOL Simultaneously

L-mode

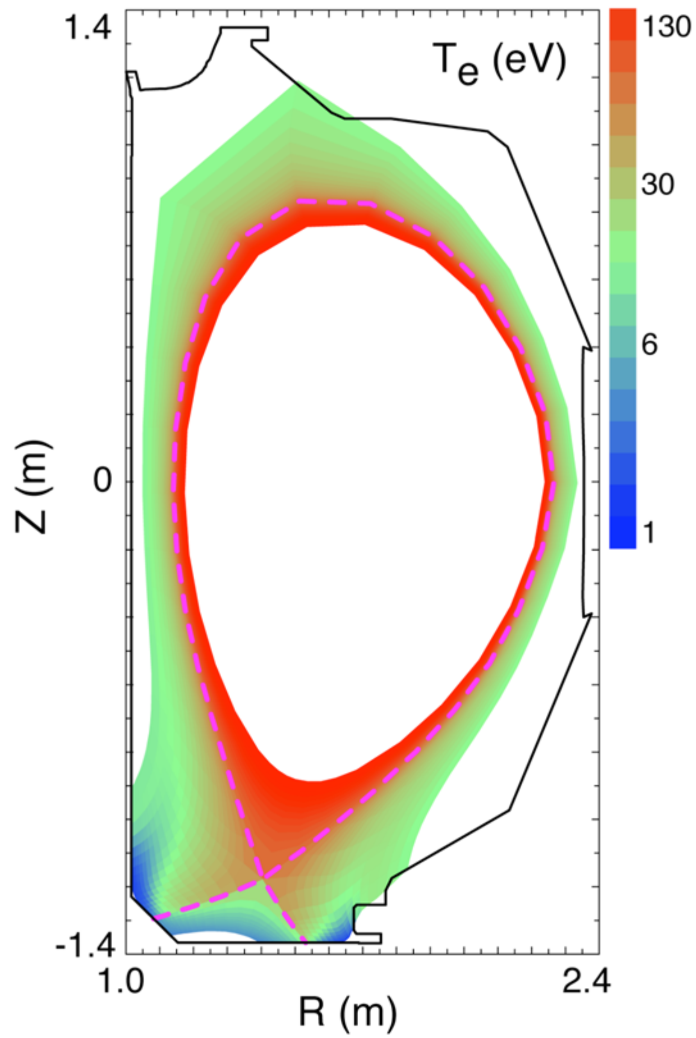

- **UEDGE predicts $T_{e,ISP}$ ~ 1.5 eV, consistent with measurements in inner divertor**
  - Inner strike point D_β/D_α ~ 0.15
  - Lack of CII emission in the inner leg
- **ExB drifts play an important role in obtaining low $T_{e,ISP}$**
  - Omitting drifts raises $T_{e,ISP}$ from 1.5 eV to 3 eV

⇒ **Less consistent with experiment!**

UEDGE Main Chamber SOL Flow is Strongly Dependent on Inner Strike Point Temperature

L-mode

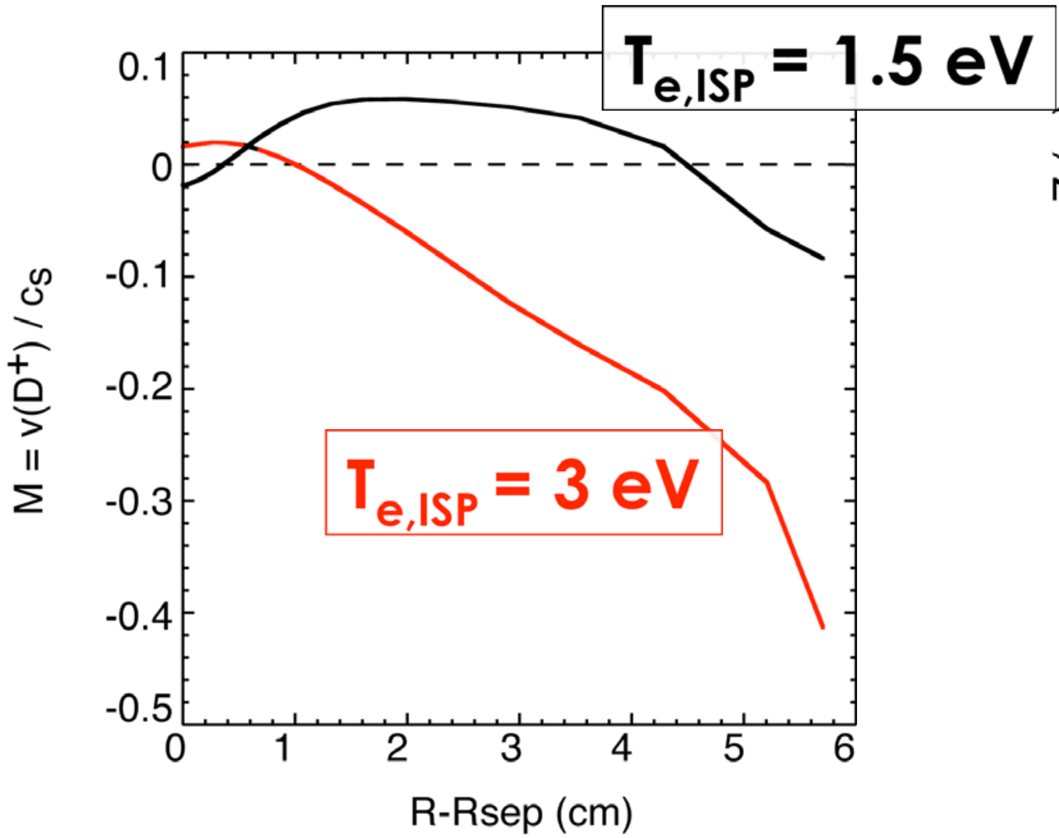

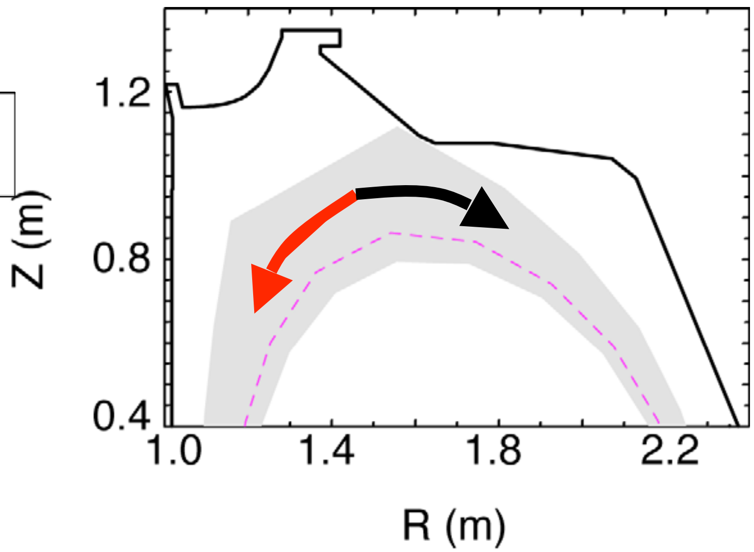

Direction of Carbon Flow in the Crown Aligned with the Deuteron Flow

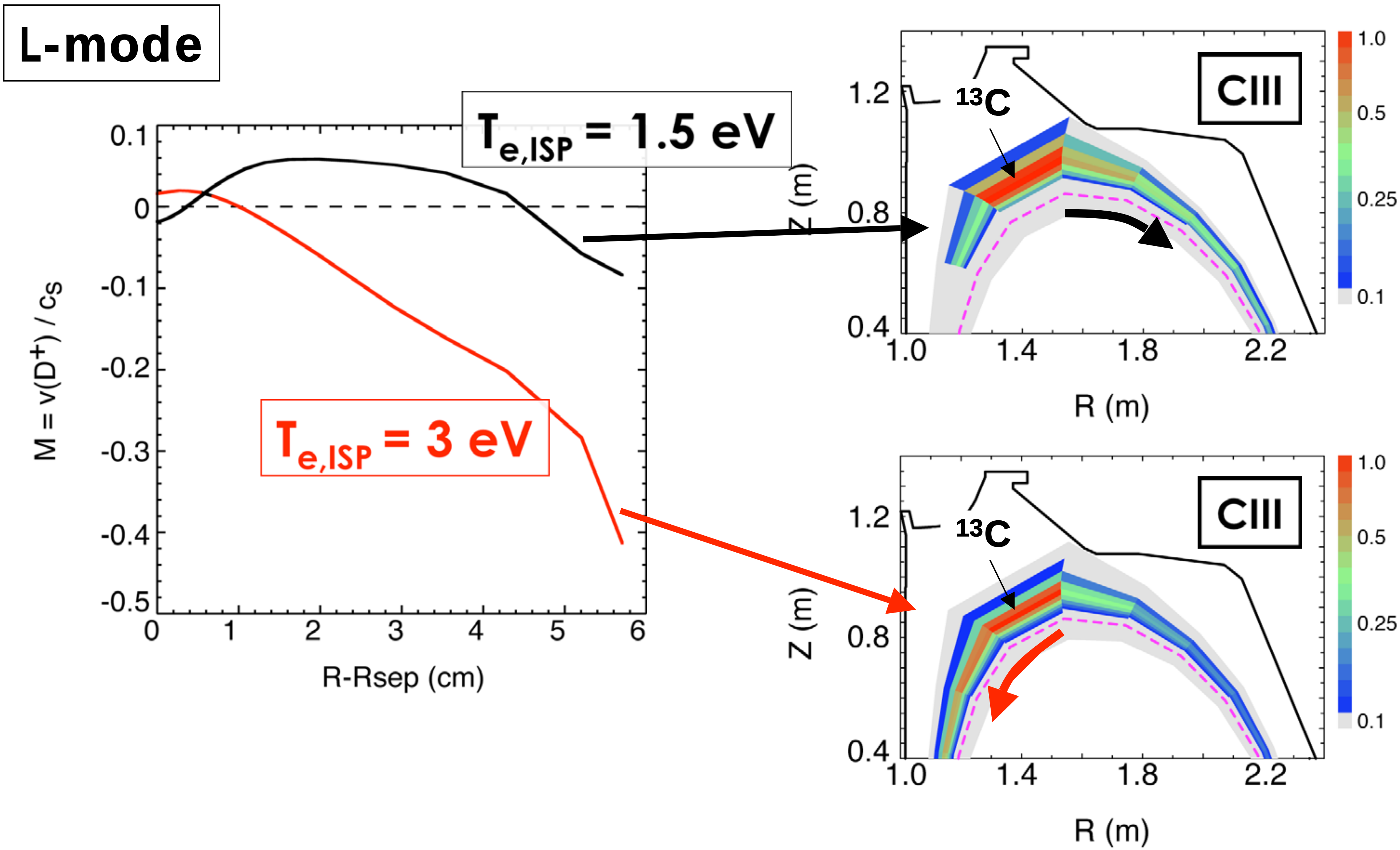

^{13}C Deposition at Inner and Outer Target is Strongly Dependent on D^+ Flow in Main SOL

L-mode

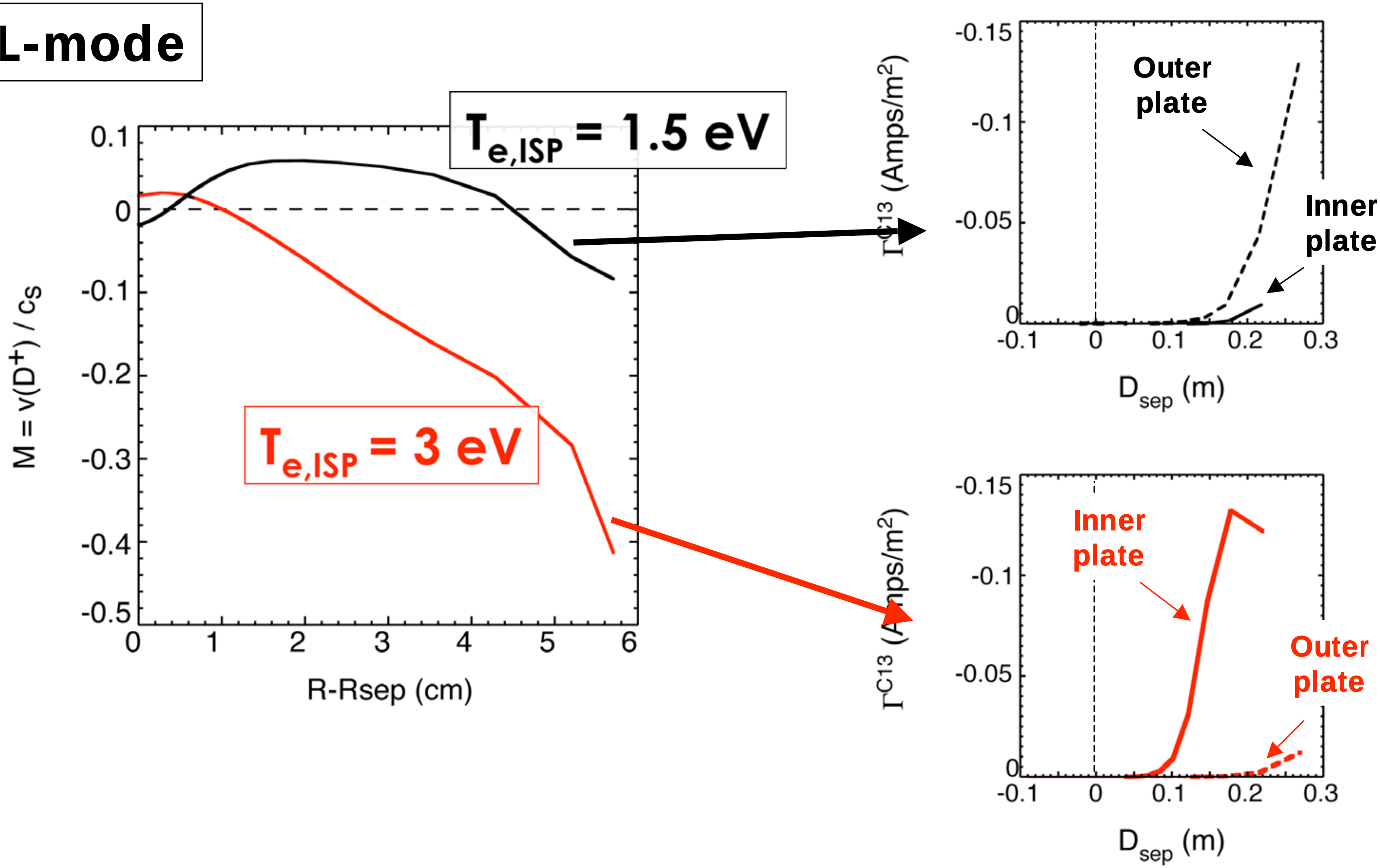

^{13}C Deposition at Inner and Outer Target is Strongly Dependent on D^+ Flow in Main SOL

L-mode

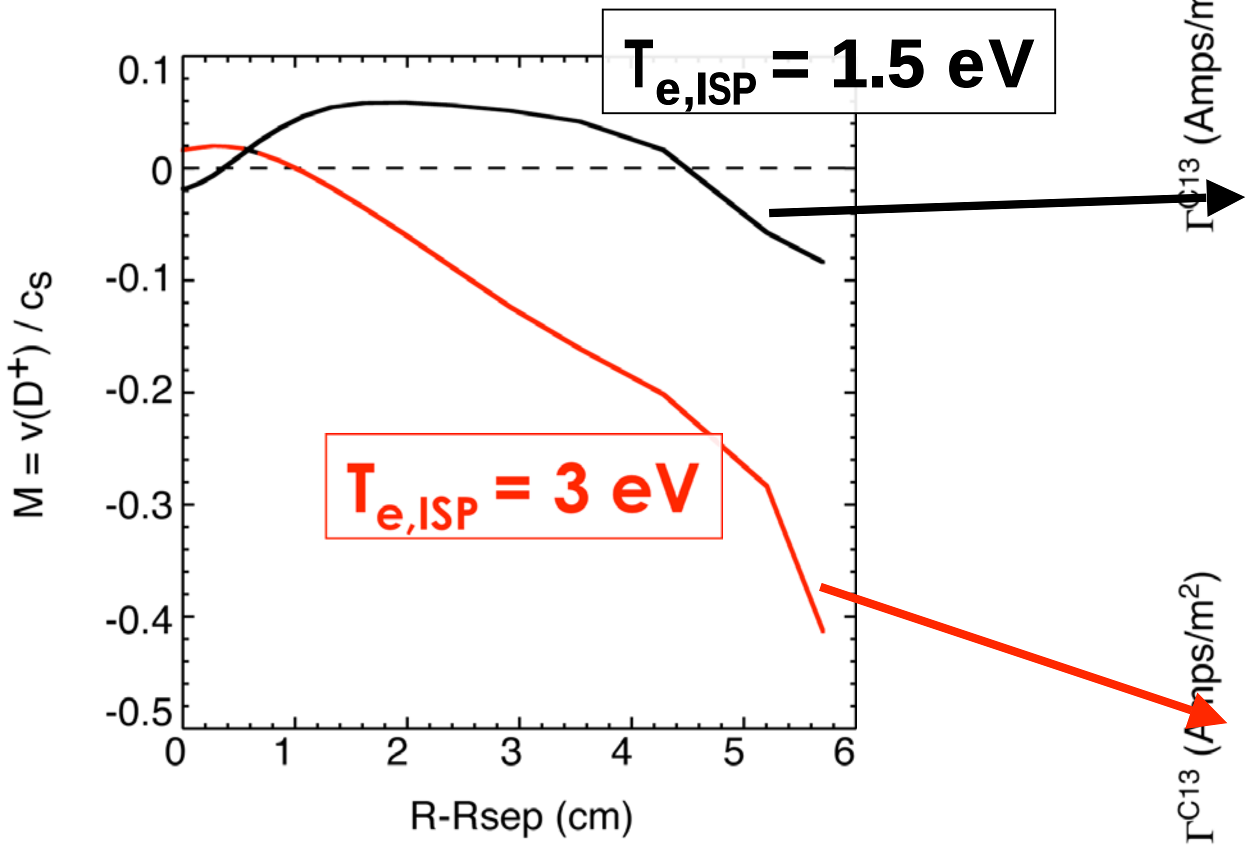

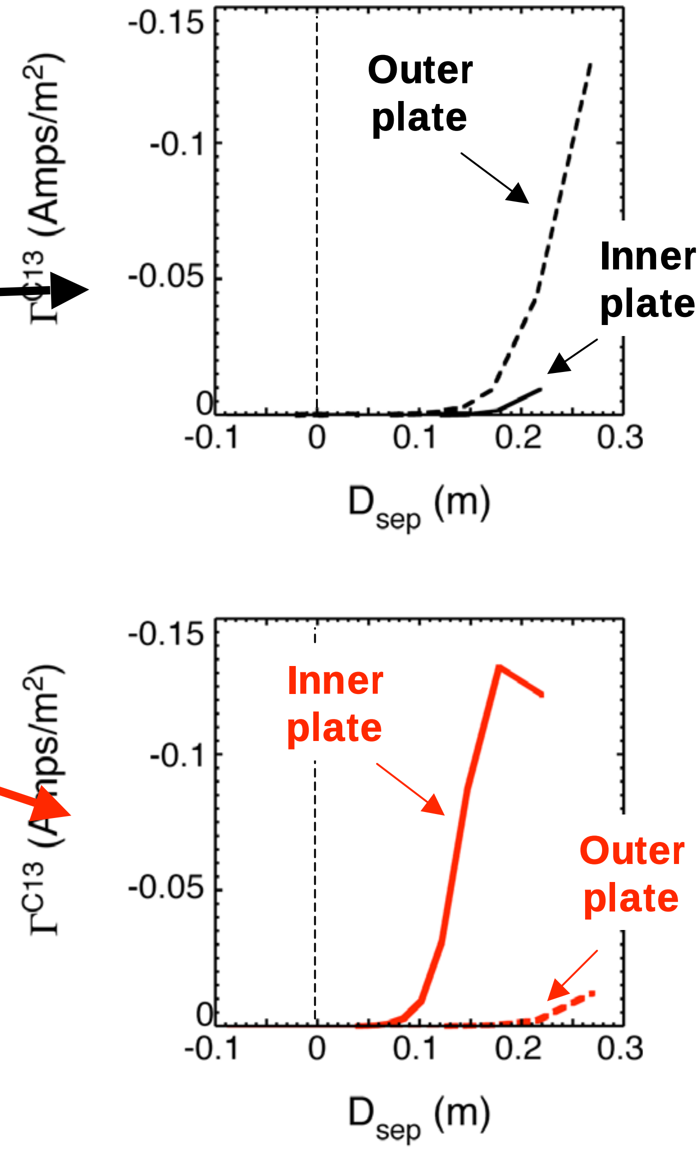

⇒ **Main chamber SOL flow and ^{13}C deposition inconsistent with low $T_{e,ISP}$**

Transport and Deposition of Carbon From the Main Chamber Walls Were Investigated in DIII-D by Methane Injection

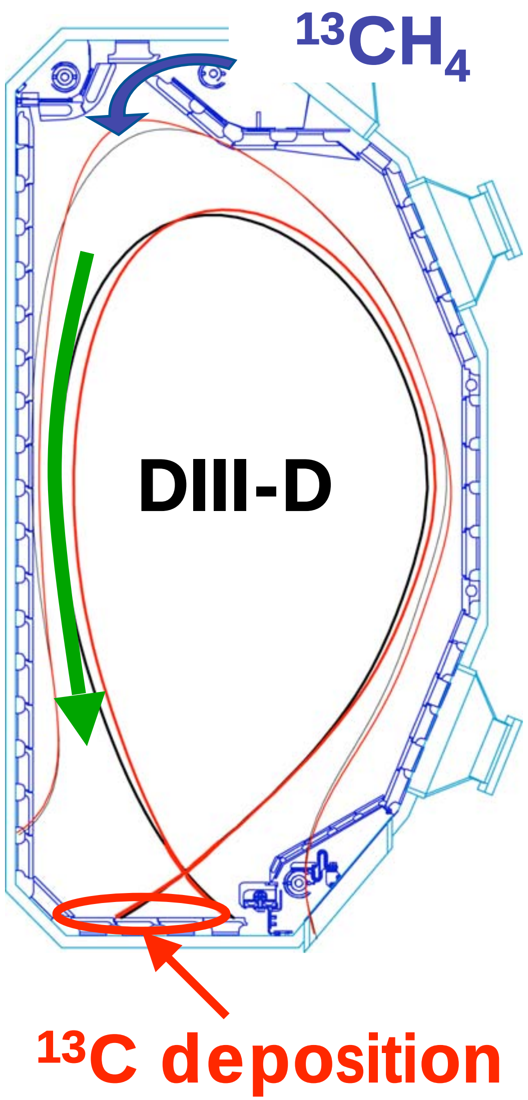

- **Toroidally symmetric $^{13}CH_4$ injection into low-density L-mode and high-density H-mode plasmas**
- **Highest ^{13}C concentration along surfaces exposed to cold divertor plasmas (T < 3 eV)**
  - Inner divertor plate in L-mode and H-mode
  - Private flux tiles in H-mode
- **Carbon transport from the crown to the inner divertor via frictional coupling to deuteron flow**
  - Deuteron flow measurements in USN plasmas
  - Carbon flow from poloidally shifted emission profiles in the crown

Predicting Tritium Retention in Future Fusion Devices With Carbon Walls Requires Further Analysis and Improved Modeling

- **50-70% of the injected ^{13}C atoms were found along plasma-facing surfaces**
  - ⇒ Accessible to surface cleanup techniques in future fusion reactor
- **Long-range migration into tile gaps, and beyond, may have occurred**
  - ⇒ Currently being assessed by surface analysis of the tile gaps
- **Improvements to predictive capability of carbon sources and deposition in tokamaks are in progress**
  - ⇒ Simultaneous simulations of multiple diagnostics measurements, including SOL flow and carbon deposition